MENTATION PAGE

Form Approved
OMB No. 0704-0188

, estimated to average 1 hour per response, including the time for reviewing instructions, searching existing data sources, g and reviewing the collection of information. Send comments regarding this burden estimate or any other aspect of this g this burden, to Washington Headquarters Services, Directorate for Information Operations and Reports, 1215 Jefferson to the Office of Management and Budget, Paperwork Reduction Project (0704-0188), Washington, DC 20503.

REPORT DATE	3. REPORT TYPE AND DATES COVERED
6-15-92	

4. TITLE AND SUBTITLE

Microwave and Infrared Dielectric Relaxation of Alkylcarbonates, Chloroform and their Mixtures at 25°C

5. FUNDING NUMBERS

DAAL03-89-K-0148

6. AUTHOR(S)

R. Chandra, Meizhen Xu, Paul Firman, Edward M. Eyring and Sergio Petrucci

7. PERFORMING ORGANIZATION NAME(S) AND ADDRESS(ES)

Weber Research Institute and Department of Chemistry, Polytechnic University, Route 110, Farmingdale, NY 11735

8. PERFORMING ORGANIZATION REPORT NUMBER

9. SPONSORING/MONITORING AGENCY NAME(S) AND ADDRESS(ES)

U. S. Army Research Office
P. O. Box 12211
Research Triangle Park, NC 27709-2211

10. SPONSORING/MONITORING AGENCY REPORT NUMBER

ARO 26636.3-CH

11. SUPPLEMENTARY NOTES

The view, opinions and/or findings contained in this report are those of the author(s) and should not be construed as an official Department of the Army position, policy, or decision, unless so designated by other documentation.

12a. DISTRIBUTION/AVAILABILITY STATEMENT

Approved for public release; distribution unlimited.

12b. DISTRIBUTION CODE

13. ABSTRACT *(Maximum 200 words)*

Microwave data yielding the complex permittivity $\epsilon^*=\epsilon'=J\epsilon''$, infrared and visible refractive indices, and infrared attenuation coefficients for liquid dimethyl-carbonate [$(CH_3O)_2CO$; abbrev:DMC], chloroform, and their mixtures have been recorded at 25°C. For pure DMC the real part of the complex permittivity ϵ' versus frequency shows two relaxation domains: the microwave frequency range interpreted as the rotational relaxation of the methoxy groups, $-OCH_3$, around the carbonyl moiety, C=O, and a newly discovered relaxation domain at infrared frequencies. The profile of n^2_{IR} (the squared refractive index) versus frequency for pure $CHCl_3$ reveals a new dielectric phenomenon hinted at by literature data obtained at far-IR frequencies. Mixtures of DMC and $CHCl_3$ have a microwave dielectric spectrum that differs markedly from that which would be expected for mole fraction $X_{DMC}=0.50$, if the two components did not interact strongly with each other. The dielectric relaxation frequencies of pure DMC and pure $CHCl_3$ are f_r=22 GHz and 27 GHz respectively. When mixed at a composition $X_{DMC}=0.50$, a dielectric relaxation spectrum is produced that can be interpreted by a Cole-Cole distribution with an average relaxation frequency f_r = 17 GHz and a distribution relaxation parameter $\alpha=0.08$ ($0<\alpha<1$ with $\alpha=0$ for a singe Debye relaxation process). This dielectric relaxation is ascribed to the formation of H-bonded complexes arising form interactions of the proton of $CHCl_3$ and the carbonyl moiety of DMC. A similar $X_{DMC}=0.50$ mixture of DMC and CCl_4 does not produce the same dielectric relaxation thus supporting the attribution of the phenomenon to the formation of a hydrogen bonded $CHCl_3$-DMC complex.

14. SUBJECT TERMS

15. NUMBER OF PAGES

16. PRICE CODE

17. SECURITY CLASSIFICATION OF REPORT	18. SECURITY CLASSIFICATION OF THIS PAGE	19. SECURITY CLASSIFICATION OF ABSTRACT	20. LIMITATION OF ABSTRACT
UNCLASSIFIED	UNCLASSIFIED	UNCLASSIFIED	UL

Microwave and Infrared Dielectric Relaxation of Alkylcarbonates, Chloroform and their Mixtures at 25°C

R. Chandra, Meizhen Xu, Paul Firman, Edward M. Eyring and Sergio Petrucci*

Weber Research Institute and Department of Chemistry, Polytechnic University, Route 110, Farmingdale, NY 11735 and Department of Chemistry, University of Utah, Salt Lake City, UT 84112

(Abstract)

Microwave data yielding the complex permittivity $\epsilon^* = \epsilon' - J\epsilon''$, infrared and visible refractive indices, and infrared attenuation coefficients for liquid dimethylcarbonate [$(CH_3O)_2CO$; abbrev:DMC], chloroform, and their mixtures have been recorded at 25°C. For pure DMC the real part of the complex permittivity ϵ' versus frequency shows two relaxation domains: the microwave frequency range previously studied and interpreted as the rotational relaxation of the methoxy groups, $-OCH_3$, around the carbonyl moiety, $>C=O$, and a newly discovered relaxation domain at infrared frequencies. This latter relaxation domain is probably attributable to some aspect of atomic polarization. The profile of n_{IR}^2(the squared refractive index) versus frequency for pure $CHCl_3$ reveals a new dielectric phenomenon hinted at by literature data obtained at far-IR frequencies. This phenomenon has been explained qualitatively by

current theories of collision induced dipoles. Mixtures of $CHCl_3$ and DMC are more interesting than mixtures of CCl_4 and DMC because of interactions in the former pair arising from H-bonding. Mixtures of DMC and $CHCl_3$ have a microwave dielectric spectrum that differs markedly from that which would be expected for mole fraction $X_{DMC} = 0.50$, if the two components did not interact strongly with each other. The dielectric relaxation frequencies of pure DMC and pure $CHCl_3$ are f_r = 22 GHz and 27 GHz respectively. When mixed at a composition $X_{DMC} = 0.50$, a dielectric relaxation spectrum is produced that can be interpreted by a Cole-Cole distribution with an average relaxation frequency f_r = 17 GHz and a distribution relaxation parameter $\alpha = 0.08$ ($0 < \alpha < 1$ with $\alpha = 0$ for a single Debye relaxation process). This dielectric relaxation is ascribed to the formation of H-bonded complexes arising from interactions of the proton of $CHCl_3$ and the carbonyl moiety of DMC. A similar $X_{DMC} = 0.50$ mixture of DMC and CCl_4 does not produce the same dielectric relaxation thus supporting the attribution of the phenomenon to the formation of a hydrogen bonded $CHCl_3$-DMC complex. Mixtures of ethylene carbonate [EC] and $CHCl_3$ up to $C_{EC} \simeq 3$ M produce a dielectric spectrum that can be interpreted as arising from hydrogen bonding between EC and $CHCl_3$.

Introduction

Correlation between chemical structure and physical phenomena as in the dielectric response of a liquid to an alternating electromagnetic wave is a challenging problem with fascinating implications. By increasing the frequency, from UHF to infrared frequencies, one may progressively freeze phenomena ranging from rotation of groups within the molecule to rotation of the whole molecule at microwave frequencies, to resonant-relaxations associated with various phenomena, widely categorized as atomic polarization. A systematic change in the chemical structure of the substance under study or of the solvent, if in liquid mixtures, may yield hints regarding the intimate nature of the relaxing phenomenon.

In the present work, we describe the microwave and infrared dielectric relaxation of dimethyl carbonate, chloroform and their mixtures. In the case of the mixtures, molecular interaction, probably through H-bonding is reflected in the dielectric relaxation process at microwave frequencies. For the pure liquids, new phenomena at infrared frequencies are observed. Comparison between the dielectric permittivity of dimethyl and ethylene carbonate reveals the role of the ring structures of ethylene carbonate in determining differences in the dielectric properties of the two compounds. Ethylene carbonate-$CHCl_3$ mixtures undergo dielectric relaxation processes at microwave frequencies assignable to H-bonding between the two components with progressive disappearance of $CHCl_3$ as an independent rotating entity with increasing concentration of ethylene carbonate.

Experimental Section

The equipment and procedure for the infrared dielectric work have been described elsewhere.[1] For the microwave work, the equipment from UHF to 90 GHz frequencies has also been described previously. We have extended the work to 127 GHz (F-band, 90 to 140 GHz), by setting up another reflectometer consisting of a Hughes impatt, square wave modulator and modulator carrier, standard directional couplers and crystal detectors. The sample cell was constructed from a precision F-band waveguide (0.040 X 0.080 inch). The cell ended in a reflector whose movements (distance from a 0.003 inch mica window at the bottom of the cell, confining the liquid) were recorded by a Mitutoyo height gauge (precision $\pm 10^{-4}$ inch) serial (S232) interfaced to a computer for movement recording. Figure 1A shows the reflected power profile of the cell filled with chloroform (and jacket thermostated at 25°C) as a function of the distance, demonstrating the excellent response of the instrument, both mechanically and in terms of only the dominant mode of the field propagating through the waveguide. Figure 1B reports the function $-\ell n\ ((\Gamma-\Gamma_\infty)/(1-\Gamma\Gamma_\infty))$ and $-\ell n\ ((\Gamma_\infty \mp \Gamma)/(1 \mp \Gamma\Gamma_\infty))$ for the maxima and the minima respectively of the power shown in Fig. 1A vs the odd and the even extrema, respectively, of the standing wave pattern. In the above Γ and Γ_∞ are the voltage reflection coefficients at distance ℓ and infinity from the mica window, defining the liquid air interface. The slope of the line obtained in Fig. 1B by linear regression corresponds to $\frac{\alpha\lambda}{2}$ while λ is obtained from the average distance of the minima or maxima, as described previously.[2] The attenuation coefficient α (cm^{-1}) and the wavelength λ in the liquid are related to the coefficients ϵ' and ϵ'' of the complex permittivity by equations (2) and (5)

(see below). The critical wavelength is given by $\lambda_c = 2b$, where b is the large dimension of the waveguide.

Dimethyl carbonate (Aldrich) was distilled after overnight exposure to P_4O_{10}; $CHCl_3$ (Aldrich) was also distilled after overnight exposure to P_4O_{10}. In both cases, P_4O_{10} was removed by decantation of the liquid before distillation. The distillation equipment was an all glass apparatus, comprising a 3 foot Vigreaux column, with ungreased joints connected instead using Teflon sleeves. Solid ethylene carbonate (Fluka) was kept in vacuo overnight, and was used without further purification. Carbon tetrachloride (Aldrich, Gold label) was purified as reported previously.[1]

Results and Calculations

For greater clarity, we will present results for the pure liquids first followed by the results for the mixtures.

(a) Dimethyl carbonate. Literature data obtained earlier in this laboratory[3] and new data in the microwave, far infrared and infrared regions for the real coefficient ϵ' of the complex permittivity $\epsilon^* = \epsilon' - J\epsilon''$, are plotted in Fig. 2 vs the frequency f expressed in Terahertz (lower abscissa) and vs the wave number $\bar{\nu}$ (cm^{-1}) for dimethyl carbonate at 25.0°C. The squared refractive index n_D^2 at the sodium doublet (λ = 589.3 nm, f = 509.1 THz, $\bar{\nu}$ = 16,969 cm^{-1}) is also reported. From the plot, two relaxation domains can be discerned. One at a lower frequency, of the Debye type, centered at f = 22 GHz (solid line in Fig 1) has been attributed to the rotation of the methoxy groups around the >C = 0 moiety (to be distinguished from the cis-trans inversion recorded[3] at f = 8.5 MHz by ultrasonic relaxation techniques at

25°C. The new far infrared, mid-infrared and visible range data show the existence of a new relaxation domain of unknown nature probably associated with some form of decay of atomic polarization of dimethyl carbonate.

Figure 3 reiterates this concept by showing the Cole-Cole plot of ϵ'' vs ϵ' for dimethyl carbonate (DMC) at 25°C. The solid line is the Debye function for a single relaxation process ending at ϵ_∞. The plot has, however, a long tail to the Debye process ending at the value of n_D^2, the permittivity at optical frequencies.

Figure 4 presents the attenuation constant α (cm^{-1}) vs both f and $\bar{\nu}$ for DMC at 25°C showing a maximum at far infrared frequencies. The various parameters ϵ', ϵ'', n^2 and α are correlated with each other by the expressions[4] valid for propagation through a fluid unconstricted by boundaries.

$$\epsilon' = \left(\frac{\lambda o}{\lambda}\right)^2 \left[1 - \left(\frac{\alpha\lambda}{2\pi}\right)^2\right] \tag{1}$$

$$\epsilon'' = \left(\frac{\lambda o}{\lambda}\right)^2 \frac{\alpha\lambda}{\pi} \tag{2}$$

$$n = \left(\frac{\epsilon'}{2}\right)^{1/2} \left\{ \left[1+\left(\frac{\epsilon''}{\epsilon'}\right)^2\right]^{1/2} + 1 \right\}^{1/2} \tag{3}$$

$$\alpha = 2\pi\bar{\nu} \left(\frac{\epsilon'}{2}\right)^{1/2} \left\{ \left[1+\left(\frac{\epsilon''}{\epsilon'}\right)^2\right]^{1/2} - 1 \right\}^{1/2} \tag{4}$$

where α is the intensity attenuation constant (cm^{-1}) related to the power attenuation constant[4] α_p by the relation $\alpha_p = 2\alpha$. From the above it is clear that for $\epsilon'' << \epsilon'$, $n^2 = \epsilon'$ and $\alpha \simeq 0$. Also for constricted propagation through rectangular waveguides[2]

$$\epsilon' = \left(\frac{\lambda o}{\lambda}\right)^2 \left[\, 1 - \left(\frac{\alpha\lambda}{2\pi}\right)^2 \,\right] + \left(\frac{\lambda_o}{\lambda_c}\right)^2 \qquad (5)$$

where the cut-off wavelength $\lambda_c = 2b$, with b the long side of the waveguide. As for the other symbols, λ_o is the free space wavelength, λ is the wavelength in the liquid at the frequency f, and $\bar{\nu} = (1/\lambda_o)$. Table I (microfilm edition) gives all the values of ϵ', ϵ'', n, and α at the frequencies f (THz) and wavenumber $\bar{\nu}$ (cm^{-1}) for DMC at 25°C. In order to avoid using ϵ_o, the static permittivity of DMC, $CHCl_3$ and their mixture in the fit of the data as an additional parameter the ϵ^o values have been determined experimentally. They are collected in Table II (microfilm edition).

b) Chloroform

Figure 5 shows the values of ϵ' vs. f (THz) and vs $\bar{\nu}$ (cm^{-1}) for pure $CHCl_3$, from microwave to visible frequencies. The data are from the literature[4] and from this laboratory. Two domains are discernible: A microwave domain, characterized by a Debye relaxation process centered at f = 27 GHz and an infrared domain. The latter involves a change of n^2 going through a maximum, as already hinted by the data of Goulon et al.[4] showing an increase of n^2 with frequency at far infrared frequencies, followed by a value of n_D^2 which was lower than the figures at far infrared frequencies[4]. A qualitative description of this change of n^2 with frequency was offered by Madden and Kivelson[5] in terms of dipole induced mechanisms.

Figure 6 shows the value of the attenuation coefficient α (cm^{-1}) vs the frequency f from the microwave to the infrared region. The data are from the literature[4] and from the present work at both microwave and infrared

frequencies. A maximum in α is discernible, although a gap from 300 to 900 GHz still exists after the combination of all the data presently available.

All the results for ϵ', ϵ'', n and α collected in our laboratory for $CHCl_3$ at 25°C are shown in Table I (microfilm edition).

c) Mixtures of DMC and $CHCl_3$ (Microwave work)

Figure 7 (microfilm edition) shows the Cole-Cole plot of ϵ'' vs ϵ' for the DMC-$CHCl_3$ mixture of composition $X_{DMC} = 0.50$ ($C_{DMC} = 5.95$ M). The dielectric loss appears altered from that expected at mole fraction $X_{DMC} = 0.50$, if the two components were not interacting with each other. The dielectric relaxation frequencies for the two pure components are $f_r = 22$ GHz for DMC and $f_r = 27$ GHz for $CHCl_3$ at 25°C. When mixed at molar ratio 1:1, a dielectric spectrum appears that can be interpreted by a Cole-Cole distribution function representing ϵ' and ϵ'' by the relation[6]

$$\epsilon' = (\epsilon_o - \epsilon_\infty) \frac{1+(f/f_r)^{(1-\alpha)} \sin(\alpha\pi/2)}{1+ 2(f/f_r)^{(1-\alpha)} \sin(\frac{\alpha\pi}{2}) + (f/f_r)^{2(1-\alpha)}} + \epsilon_\infty \qquad (6)$$

$$\epsilon'' = (\epsilon_o - \epsilon_\infty) \frac{(f/f_r)^{(1-\alpha)} \cos(\alpha\pi/2)}{1+2(f/f_r)^{(1-\alpha)} \sin(\frac{\alpha\pi}{2}) + (f/f_r)^{2(1-\alpha)}} \qquad (7)$$

where ϵ_o and ϵ_∞ are the dielectric perimittivities at low and high frequencies with respect to the average relaxation frequency f_r (f_r= 17 GHz) and α is the distribution relaxation parameter ($\alpha = 0.08$), with $0<\alpha<1$. For α=0, functions 6 and 7 reduce themselves to a pure Debye function. The relaxation parameters ϵ_o, ϵ_∞, f_r and α used to fit the data at all the compositions investigated for the DMC-$CHCl_3$ mixtures at 25°C are shown in Table III (microfilm edition). The fit by equations 6 and 7, judged by the expression ($\Sigma|\epsilon'_{calc} - \epsilon'_{exp}| + \Sigma|\epsilon''_{calc} - \epsilon''_{exp}|$), is better than that obtained using a pure Debye function.

The proposed physical interpretation of the appearance of a narrow Cole-Cole distribution function with an average relaxation frequency lower than those of the two pure components, is in terms of the formation of hydrogen bonds between the proton of $CHCl_3$ and the $\rangle C = O$ moiety of DMC, forming molecular complexes. The appearance of a distribution function presumably reflects the many molecular configurations contributing (by the relaxation of molecular motions) to the spectrum. Figure 8 (microfilm edition) is a Cole-Cole plot for the mixture DMC-CCl_4 of composition $X_{DMC} = 0.50$ at 25°C. It is significant that this mixture does not reveal the same dielectric phenomenon shown for the chloroform mixtures, thus suggesting that the broadening of the dielectric spectra of DMC-$CHCl_3$ mixtures at microwave frequencies is attributable to the presence of the proton of $CHCl_3$. We notice that for the DMC-CCl_4 mixture of $X_{DMC} = 0.50$, the relaxation frequency is $f_r = 22$ GHz as in pure DMC and that, within experimental error, the dielectric losses can be interpreted by a single Debye process (Fig. 8, microfilm edition). On the contrary, for the DMC-$CHCl_3$ mixtures, the average relaxation time $\tau_D = (2\pi f_r)^{-1}$ goes through a broad maximum with composition when plotted vs X_{DMC} at 25°C (Fig 9A). The two ordinates at $X_{DMC} = 0$ and $X_{DMC} = 1$ report the dielectric relaxation time of chloroform and of DMC respectively at 25°C.

Figure 9B shows the relaxation strength $(\epsilon_o - \epsilon_\infty)$ vs the composition, expressed in mole fraction X_{DMC}, for the DMC-$CHCl_3$ mixture at 25°C. A linear relation can describe the data within experimental error supporting the interpretation given above in terms of a continuous distribution of relaxation times reflecting many possible configurations. Should one configuration (such

as a 1:1 complex) be predominant, some singularity in the quantity $(\epsilon_o - \epsilon_\infty)$ vs. composition would be expected.

d) Mixtures of DMC-CCl_4 and DMC-$CHCl_3$ at $X_{DMC} = 0.50$ (Far infrared work)

We reported in Fig. 4 above the attenuation coefficient α (cm^{-1}) vs frequency f and wavenumber $\bar{\nu}$ for pure DMC at 25°C showing a maximum at $\bar{\nu} \simeq$ 135-140 cm^{-1}. Since the molecular nature of the phenomenon is not known, we have explored whether it would be affected by molecular interactions arising from hydrogen bonding as reflected in the microwave region. To this end we have investigated two mixtures: 1) DMC-CCl_4 at $X_{DMC} = 0.51$ and DMC-$CHCl_3$ at $X_{DMC} = 0.49$ in the far infrared region. Table I and Figs. 10A and 10B present the attenuation constants α (cm^{-1}) vs the frequency f (THz) and wavenumber $\bar{\nu}$ (cm^{-1}) encompassing the entire region from microwave (f = 13 GHz) to mid infrared frequencies (f = 101 THz, or $\bar{\nu} = 3367$ cm^{-1}). For both systems, the data are the same within experimental error for α ($\simeq$ 10%), and the peak appears unshifted within experimental error with respect to the peak for pure DMC. These results seem to point to an intramolecular process which is sensitive neither to dilution as in the CCl_4 nor to intermolecular interaction as when DMC is dissolved in $CHCl_3$. It is possible that the process is related to some intramolecular distortion of DMC, part of the atomic polarization phenomena in this region of the electromagnetic spectrum.

e) Mixtures of Ethylene Carbonate and $CHCl_3$

It was suggested[3] that the dramatic differences in static permittivity between the cyclic carbonates such as propylene carbonate, ethylene carbonate (above its melting point) and the acyclic DMC is probably due to the preponderant trans configuration of the methoxy groups of the DMC.

In order to draw structural comparisons it is necessary to extend some of the above work to one of the cyclic carbonates. Ethylene carbonate is the most appealing one since it is structurally the closest to DMC, with the exception of the ethylene moiety instead of the two methyl groups connected to the carbonate group. Ethylene carbonate is soluble in $CHCl_3$ (but not in CCl_4, at least to an extent that would be useful at compositions employed in this work). Four mixtures in a relatively dilute range (compared to those involving DMC) from 0.5 to 3.0 M have been investigated from 1.1 MHz (static range) to optical frequencies. We report ϵ', ϵ'', the refractive index n, where measurable in the IR region, and the attenuation constant α. For the composition C_{EC} = 3.01 M the presence of a maximum in α at $\bar{\nu} \simeq 210$ cm^{-1}, already found by Durig et al.[7] in benzene solutions at $\bar{\nu} \simeq 217$ cm^{-1}, has been confirmed. The data for ϵ', ϵ'' and n in the microwave and infrared regions investigated are reported in Table I for the various mixtures of ethylene carbonate-$CHCl_3$ at 25°C. The infrared absorption coefficients α in the far IR region are also reported in Table I (microfilm edition) up to the concentration C_{EC} = 3.01 M. The static permittivities ϵ_o, measured at 1.1 MHz and 25°C for mixtures of ethylene carbonate-$CHCl_3$ in all the composition range measurable, up to saturation, are reported in Table II (microfilm edition). The microwave data for the above mixtures, together with the static permittivities can be described best by the sum of two Debye relaxation functions

$$\epsilon' = (\epsilon_o - \epsilon_{\infty 1}) \frac{1}{1+(f/f_I)^2} + (\epsilon_{\infty 1} - \epsilon_{\infty 2}) \frac{1}{1+(f/f_{II})^2} + \epsilon_{\infty 2} \qquad (8)$$

$$\epsilon'' = (\epsilon_o - \epsilon_{\infty 1}) \frac{(f/f_I)}{1+(f/f_I)^2} + (\epsilon_{\infty 1} - \epsilon_{\infty 2}) \frac{(f/f_{II})}{1+(f/f_{II})^2} \qquad (9)$$

up to C_{EC} = 2.0 M, whereas at C_{EC} = 3.0 M a single Debye relaxation suffices to describe the data. This is illustrated in Fig. 11 where the Cole-Cole plots of ϵ'' vs ϵ' for the mixtures of molarity C_{EC} = 0.529, C_{EC} = 1.00, C_{EC} = 2.00 and C_{EC} = 3.01 M are reported at 25°C.

The parameters ϵ_o (interpolated from the measured ϵ_o values), $\epsilon_{\infty 1}$, $\epsilon_{\infty 2}$, f_I and f_{II}, used to fit the microwave data are presented in Table III (microfilm edition).

From Fig. 11 it is evident that the relaxation at lower frequency with relaxation strength $(\epsilon_o - \epsilon_\infty)$ increases in strength, with increasing concentration of ethylene carbonate, up to complete annexation of the upper relaxation process, characterized by the relaxation strength $(\epsilon_{\infty 1} - \epsilon_{\infty 2})$ at C_{EC} = 3.0 M. Furthermore, the position of the upper relaxation frequency f_2 averages 30 GHz which is close enough to the reported relaxation of pure $CHCl_3$, f_r = 27 GHz, to tentatively assign the upper relaxation process to the rotational relaxation of $CHCl_3$ in the mixture. An indication of the meaning of the lower relaxation process, due to ethylene carbonate in the mixture, can be obtained by applying the Böttcher function

$$(\epsilon_o - \epsilon_{\infty 1}) = \frac{4\pi \, L \times 10^{-3} C_{EC}}{(1 - \alpha f)^2} \, \frac{3\epsilon_o}{2\epsilon_o + 1} \, \frac{\mu^2}{3kT}$$

to the present data. In Fig. 11 the quantity $\phi(\epsilon) = (\epsilon_o - \epsilon_{\infty 1}) \, \frac{2\epsilon_o + 1}{3\epsilon_o}$ is plotted vs the concentration of ethylene carbonate C_{EC} (mol/dm^3). By neglecting the product of the polarizability α and the internal field factor f (since (1-αf) is of the order of 0.9), the slope of $\phi(\epsilon)$ vs C_{EC} as reported in Fig. 11, leads to an average apparent dipole moment $\mu = 8.1 \times 10^{-18}$ esu cm. This number appears to be large compared to the value used[8] for the vapor

phase μ_v = 5.1 D (1D = 10^{-18} esu cm) for propylene carbonate, and taken to be 3% higher than the value reported for propylene carbonate in benzene solutions.[9] However, it was suggested[10] that the effective molecular electric moment μ within a polar liquid is related to the dipole moment μ_v of the isolated molecule in the vapor phase by the Onsager expression[11]

$$\mu = \mu_v \frac{(n^2 + 2)\ (2\ \epsilon_o + 1)}{3\ (2\ \epsilon_o + n^2)}$$

with n the low frequency limit of the refractive index, in principle corresponding to the square root of the high frequency limiting permittivity.[8] For propylene carbonate at 20°C n_D = 1.42166.[8] By using[8] n = 1.1 n_D = 1.5638, namely n^2 = 2.45, one calculates for propylene carbonate μ = 7.48 D, a value comparable to the μ = 8.1 D obtained for ethylene carbonate in $CHCl_3$. The finding that the rotational relaxation of $CHCl_3$ appears to be swamped by the increasing losses of the relaxation process relaxing at lower frequencies (as Fig. 11, according to the numerical fit, seems to reveal), can be ascribed to hydrogen bonding between the two components of the mixture. In other words, because of hydrogen bonding between ethylene carbonate and chloroform, the latter ceases to exist in solution as a separately rotating entity, as the concentration of ethylene carbonate is increased. In particular, chloroform in the mixture with ethylene carbonate where C_{EC} = 3.01 M, has a molarity C_{chl} = 10.14 M, namely 3.4 times larger than C_{EC} = 3.01. At this composition the Cole-Cole locus shows a disappearance of the chloroform contribution to the locus according to the two Debye relaxation fit. A ratio of about three could be justified by a model envisaging three hydrogen bonds between three

chloroform molecules and an ethylene carbonate molecule, occurring through the three atoms of the carbonate group. The above can be paraphrased by calling $\mu^2 = g\mu_v^2$ in the Böttcher equation where μ_v is the dipole moment of the isolated noninteracting ethylene carbonate molecule taken to be $\mu_v \simeq 5$ D, similar to the value for propylene carbonate[8,9] and g is the Kirkwood parameter reflecting molecular association. For $\mu = 8.1$ D as for ethylene carbonate in chloroform at $C_{EC} \leq 3$ M, from $\mu^2 = g\,\mu_v^2$, it would result that g = 2.6, a value that is not far from the one envisaged by the above speculative model.

Acknowledgement. Support of this work by the Army Research Office, Research Triangle Park, NC, through Grant DAAL03-89-K-0148 is gratefully acknowledged.

References

1. Firman, P.; Marchetti, A.; Xu, M.; Eyring, E.M.; Petrucci, S. J. Phys. Chem. *1991*, 95, 7055.

2. Farber, H.; Petrucci, S. in The Chemical Physics of Solvation Dogonadze, R. R. et al., Eds.; Elsevier, Amsterdam, *1986*; Vol. B. Chapter 8.

3. Saar, D.; Brauner, J.; Farber, H.; Petrucci, S. J. Phys. Chem. *1978*, 82, 2531.

4. Goulon, J.; Rivail, J. L.; Fleming, J. W.; Chamberlain, J.; Chantry, G. W.; Chem. Phys. Lett. *1973*, 18, 211.

5. Madden, P.; Kivelson, D. in Advances in Chemical Physics, Prigogine, I., Rice, S. A., eds.; J. Wiley and Sons, N.Y., *1984*, Vol. LVI.

6. Hill, N. in Dielectric Properties and Molecular Behaviour, Hill, N. et al., Eds., Van Nostrand Reinhold, London, *1969*.

7. Durig, J. R., Coulter, G. L.; Wertz, D. W. J. Mol. Spectr. *1968*, 27, 285.

8. Cavell, E. A. S. J. Chem. Soc. Farad. Trans II *1974*, 70, 78.

9. Kempa, R. F.; Lee, W. H. J. Chem. Soc. *1961*, 100 and literature cited therein.

10. Harris, F. E.; Alder, B. J. J. Chem. Phys. *1953*, 21, 1031.

11. Onsager, L. J. Am. Chem. Soc. *1936*, 58, 1486.

Table I

Experimental values of ϵ', ϵ'', n and α at the frequencies f(THz) and wavenumbers $\bar{\nu}(cm^{-1})$ for the systems investigated at 25°C.

DMC

f(THz)	$\bar{\nu}(cm^{-1})$	ϵ'	ϵ''	n	$\alpha(cm^{-1})$
0.60×10^{-3}	0.020	3.08[a]	0.055[a]		0.00198
0.90×10^{-3}	0.030	3.15[a]	0.055[a]		0.00296
1.20×10^{-3}	0.040	3.11[a]	0.05[a]		0.00349
1.50×10^{-3}	0.050	3.12[a]	0.08[a]		0.00743
4.0×10^{-3}	0.133	3.06[a]	0.16[a]		0.037_4[b]
$8.5_1 \times 10^{-3}$	0.284	3.01	0.28[a]		0.141[b]
16.3×10^{-3}	0.546	2.84[a]	0.39[a]		0.408[b]
33.7×10^{-3}	1.12	2.62[a]	0.38[a]		0.875[b]
50.3×10^{-3}	1.68	2.52	0.30		1.127
66.6×10^{-3}	2.22	2.49[a]	0.25[a]		1.137[b]
66.6×10^{-3}	2.22	2.51[a]	0.24[a]		1.184[b]
89.1×10^{-3}	2.97	2.39	0.206		1.324
126.7×10^{-3}	4.22	2.38	0.184		1.619
126.5×10^{-3}	4.22	2.37	0.180		1.577
15.30	510			1.513	7.85
21.15	705			1.496	4.66
70.50	2350			1.379	9.78
100.5	3350			1.382	4.83
114.0	3800			1.383	2.60
138.0	4600			1.355	3.47
145.5	4850			1.365	0.847
509.08	16,969			1.3666[b']	

[a] Values taken from the literature: Saar D. et al., J. Phys. Chem. 1978, 82, 2531.

[b] The values of α are the experimental values. Notice that eqs. 3 and 4 are consistent with equations 1 and 2, but not with eq. 5 including the term $(\lambda_o/\lambda_c)^2$ in ϵ', necessary for waveguide work.

[b'] Value of n_D at the sodium doublet in the visible.

Table I (continued)

DMC

Additional values of the attenuation coefficient $\alpha(cm^{-1})$, in the far-IR and IR region encompassing the observed maximum in α.

f(THz)	$\bar{\nu}(cm^{-1})$	$\alpha(cm^{-1})^c$
2.26	75.2	10.4
2.39	79.7	18.0 ± 1.7
2.70	90	25.3 ± 3.4
3.00	100	30.7 ± 0.2
3.14	104.8	34.1 ± 1.5
3.30	109.9	43.6
3.45	115.1	55.9 ± 1.6
3.60	120	65.8 ± 2.5
5.09	170	58.2
5.71	190.3	46.8
6.00	200	41.1 ± 1.0
14.1	470	$7.8_5{}^d$
69.0	2300	$6.2_2{}^d$
100.5	3350	$4.6_3{}^d$
114.0	3800	$2.3_7{}^d$
138.0	4600	$3.1_7{}^d$
145.5	4850	$0.78_1{}^d$

[c] A second run was performed at spot frequencies also with a Si windowed variable path cell in the far-IR region and the data averaged as indicated. The average $\pm(\Delta\alpha/\alpha)\% = 6$. The data for α corresponding to α >70 cm^{-1} between 120 and 170 cm^{-1} have been omitted because they were judged to be unreliable.

[d] Third run with KRS5 windowed variable path cell.

Table I (continued)

$CHC\ell_3$

f(THz)	$\bar{\nu}(cm^{-1})$	ϵ'	ϵ''	n	$\alpha(cm^{-1})$
0.355×10^{-3}		4.84	0.035		5.9×10^{-4}
0.50×10^{-3}		4.81	0.052		0.0125
1.80×10^{-3}		4.76	0.14		0.0121
2.32×10^{-3}		4.67	0.21		0.0241
3.32×10^{-3}		4.88	0.33		0.0521
8.32×10^{-3}		4.55	0.81		0.353
13.75×10^{-3}		4.11	0.96		0.719
29.63×10^{-3}		3.38	1.17		2.10
50.70×10^{-3}		2.86_5	1.04_5		3.60
88.82×10^{-3}		2.49	0.77		4.75
126.9×10^{-3}		2.32	0.56		4.94
4.35	145			1.46_2	
4.80	160			1.50_1	
7.74	258			1.52_4	
14.00	467			1.56_9	
14.10	470			1.53_7	0.91
32.25	1075			1.59_2	0.75
39.90	1330			1.548	
54.00	1800			1.459	0.20
102.0	3400			1.441	0.24
120.0	4000			1.439	0.40
138.0	4600			1.428	0.072
32.2*	1074			1.586	0.75
32.3*	1078			1.591	0.75
40.0*	1333			1.533	
54.1*	1803			1.433	0.20
102.2*	3407			1.432	0.24
120.6*	4020			1.438	0.40
136.4*	4547			1.423	0.072
509.08	16,969			1.4432[b]	

* 2nd Run

Table I (continued)

$CHCl_3$

Additional values of the attenuation coefficient $\alpha(cm^{-1})$[f]

f(THz)	$\bar{\nu}(cm^{-1})$	$\alpha(cm^{-1})$
2.40	80	5.81
2.70	90	3.86
3.00	100	4.27
3.30	110	2.12
4.50	150	1.96
5.40	180	1.34
6.60	220	1.37
9.00	300	1.51
9.60	320	1.08
9.60	320	1.27
9.99	333	1.09
12.75	425	1.10
13.50	450	0.88
13.50	450	1.09
14.10	470	0.98
16.50	550	0.40
16.50	550	0.42
54.00	1800	0.30
78.00	2600	0.11
78.00	2600	0.10

[f] Data obtained during additional runs performed with variable path cells equipped with either KRS5 windows (above 300 cm^{-1}) or Si windows.

Table I (continued)

DMC - $CHCl_3$ mixture X_{DMC} = 0.268 C_{DMC} = 3.23 M

f(THz)	$\bar{\nu}(cm^{-1})$	ϵ'	ϵ''	n	$\alpha(cm^{-1})$
0.466×10^{-3}		4.24	0.0658		0.00155
0.615×10^{-3}		4.23	0.0720		0.00225
0.860×10^{-3}		4.20	0.0740		0.00325
1.80×10^{-3}		4.20	0.260		0.0239
2.64×10^{-3}		4.15	0.269		0.0365
3.40×10^{-3}		4.18	0.372		0.0654
8.32×10^{-3}		3.91	0.736		0.352
13.75×10^{-3}		3.56	0.843		0.686
29.68×10^{-3}		2.97	0.893		1.74
50.3×10^{-3}		2.66	0.750		2.73
88.7×10^{-3}		2.44	0.489		3.08
126.8×10^{-3}		2.36	0.406		3.56
8.568	319			1.579	9.87
13.50	450			1.523	3.98
100.9	3364			1.455	1.47
116.0	3865			1.442	1.08
140.0	4666			1.431	0.433
146.3	4875			1.416	0.238
509.08	16,969			1.4202	

Table I (continued)

DMC-$CHC\ell_3$ mixture. $X_{DMC} = 0.49_4$ $C_{DMC} = 5.95$ M

f(THz)	$\bar{\nu}(cm^{-1})$	ϵ'	ϵ''	n	α
0.464×10^{-3}		4.11	0.126		0.0030
0.615×10^{-3}		4.00	0.086		0.0028
0.860×10^{-3}		4.04	0.146		0.0066
1.80×10^{-3}		4.03	0.214		0.021
2.20×10^{-3}		4.09	0.206		0.023_5
3.12×10^{-3}		3.99	0.361		0.059
8.32×10^{-3}		3.62	0.681		0.340
13.75×10^{-3}		3.26	0.736		0.629
29.61×10^{-3}		2.77	0.625		1.27_6
50.30×10^{-3}		2.62	0.554		2.05_2
88.61×10^{-3}		2.43	0.359		2.27_6
126.7×10^{-3}		2.36	0.29_5		2.58_8
14.90	496			1.532	8.16_3
101.36	3379			1.409	3.01
115.59	3853			1.404	1.95
142.65	4755			1.386	1.29
509.08	16,969			1.4015	

Table I (continued)

DMC-$CHC\ell_3$ X_{DMC} = 0.491 C_{DMC} = 5.86 M

(Additional values of the attenuation coefficient $\alpha(cm^{-1})$ in the far IR region encompassing the maximum in attenuation).

f(THz)	$\bar{\nu}(cm^{-1})$	$\alpha(cm^{-1})$
1.95	64.93	6.31
2.39	79.71	12.88
2.70	90.0	15.64
3.30	109.9_2	24.74
3.45	115.0_7	37.02
3.61	120.2_1	52.47
3.74	124.71	61.15
4.05	135.00	71.83
4.20	140.14	71.77
4.36	145.28	70.51
4.49	149.78	67.85
4.65	154.92	52.12
4.80	160.07	46.19
5.09	169.71	41.94
5.40	180.00	31.70
5.71	190.28	19.95

Table I (continued)

DMC-$CHCl_3$ mixture X_{DMC} = 0.781, C_{DMC} = 9.25M

f(THz)	$\bar{\nu}(cm^{-1})$	ϵ'	ϵ''	n	$\alpha(cm^{-1})$
0.466		3.58	0.0342		0.00088
0.615		3.53	0.0427		0.00147
0.860		3.56	0.0621		0.00248
1.80		3.44	0.160		0.0163
2.31		3.58	0.177		0.0227
2.68		3.48	0.207		0.0312
3.40		3.45	0.249		0.0476
8.32		3.31	0.468		0.248
13.75		3.04	0.534		0.478
29.65		2.66	0.526		1.10_5
49.80		2.47	0.402		1.54
88.69		2.35	0.262		1.69
126.7		2.36	0.222		1.95
9.60	320				20.8_6
13.90	464			1.539	7.90
101.0	3367			1.397	3.73
107.9	3598			1.384	4.73
114.2	3808			1.417	2.87
144.2	4808				1.15
509.08	16969			1.3813	

Table I (continued)

DMC-$CC\ell_4$ mixture $X_{DMC} = 0.51$ $C_{DMC} = 5.60$

f(THz)	$\bar{\nu}(cm^{-1})$	ϵ'	ϵ''	n	$\alpha(cm^{-1})$
0.464×10^{-3}		2.61	0.14_5		0.00043_6
0.615×10^{-3}		2.58	0.019		0.00075_1
0.860×10^{-3}		2.60	0.032		0.0018_1
$3.40_5 \times 10^{-3}$		2.57	0.055_7		0.012_4
8.32×10^{-3}		2.52	0.13_5		0.085_2
$13.7_5 \times 10^{-3}$		2.46	0.14_8		0.15_2
29.67×10^{-3}		2.36	0.16_3		0.37_2
50.35×10^{-3}		2.31	0.13_1		0.53_3
88.46×10^{-3}		2.28	0.10_0		0.65_5
126.28×10^{-3}		2.29	0.084		0.74_4
6.00	200			1.522	17.8_1
15.00	500			1.525	6.82_9
20.25	675			1.514	4.68
69.00	2300			1.443	3.68
100.5	3350			1.413	2.08
114.0	3800			1.417	1.51
141.7	4725			1.406	1.44
509.08	16969			1.4116_5[b]	

Table I (continued)

DMC-$CC\ell_4$ mixture $X_{DMC} = 0.509$ $C_{DMC} = 5.60$ M

Additional values of the attenuation coefficient $\alpha(cm^{-1})$ in the far-infrared region showing a maximum in α.

f(THz)	$\bar{\nu}(cm^{-1})$	$\alpha(cm^{-1})$
2.70	90.0	12.11
3.01	100.28	15.24
3.30	109.93	21.86
3.61	120.21	40.83
3.74	124.71	53.14
3.90	129.85	75.99
4.05	135.00	75.02
4.20	140.14	68.40
4.49	149.78	53.94
4.65	154.92	49.81
4.80	160.07	42.78
5.11	170.35	33.80
5.71	190.27	18.07
6.00	199.92	18.23

Table I (continued)

Ethylene carbonate - $CHC\ell_3$ mixture $X_{EC} = 0.0423$ $C_{EC} = 0.529$ M

f(THz)	$\bar{\nu}(cm^{-1})$	ϵ'	ϵ''	n	$\alpha(cm^{-1})$
0.297×10^{-3}		7.21	0.14		0.00157
0.466×10^{-3}		7.12	0.20		0.0038
0.615×10^{-3}		7.09	0.28		0.0067
0.860×10^{-3}		7.04	0.38		0.0128
1.36×10^{-3}		6.93	0.60		0.032
1.80×10^{-3}		6.97	0.85		0.061
2.24×10^{-3}		6.92	1.03		0.092
2.69×10^{-3}		6.94	1.04		0.110
3.39×10^{-3}		6.91	1.25		0.168
8.32×10^{-3}		5.52	2.06		0.794
13.75×10^{-3}		4.74	2.05		1.390
29.64×10^{-3}		3.57	1.67		2.857
55.36×10^{-3}		3.10	1.33		4.67
55.23×10^{-3}		2.88	1.27		4.62
88.56×10^{-3}		2.61	0.97		5.79
126.6×10^{-3}		2.46	0.70		5.96
126.6×10^{-3}		2.43	0.71		6.15
4.80	160			1.482	1.808
14.40	480			1.573	2.353
64.5	2150			1.449	0.811
82.5	2750			1.440	0.838
100.5	3350			1.451	0.342
115.5	3850			1.457	0.452
122.7	4090			1.430	0.632
132.0	4400			1.444	0.626
140.3	4675			1.441	2.6×10^{-3}
509.08	16969			1.4435	

Table I (continued)

Ethylene carbonate - $CHC\ell_3$ mixture $X_{EC} = 0.0789$ $C_{EC} = 1.00$ M

f(THz)	$\bar{\nu}(cm^{-1})$	ϵ'	ϵ''	n	$\alpha(cm^{-1})$
0.297×10^{-3}		9.53	0.23_4		0.0024
0.466×10^{-3}		9.30	0.34_0		0.0054
0.615×10^{-3}		9.26	0.39_7		0.0084
0.86×10^{-3}		9.05	0.63_4		0.0190
1.30×10^{-3}		9.13	1.08		0.0486
1.80×10^{-3}		9.07	1.38		0.0862
2.25×10^{-3}		8.96	1.67		0.131
3.42×10^{-3}		8.77	2.23		0.267
8.32×10^{-3}		6.41	3.31		1.15
$13.7_5 \times 10^{-3}$		4.93	2.86		1.87
$29.6_3 \times 10^{-3}$		3.76	2.16		3.54
$55.2_8 \times 10^{-3}$		2.97	1.41		5.02
$88.7_3 \times 10^{-3}$		2.73	1.15		6.66
126.9×10^{-3}		2.49	0.79		6.67
126.6×10^{-3}		2.45	0.89		7.57
4.80	160			1.483	3.513
7.50	250			1.496	6.845
14.40	480			1.565	3.823
14.79	493			1.568	3.823
100.3_5	3345			1.441	0.455
100.5	3351			1.417	0.455
115.6	3854			1.450	0.546
132.1_5	4405			1.449	0.900
140.1	4670			1.423	
509.1	16969			1.4439	

Table I (continued)

Ethylene carbonate - $CHCl_3$ mixture $X_{EC} = 0.156$ $C_{EC} = 2.00$ M

f(THz)	$\bar{\nu}(cm^{-1})$	ϵ'	ϵ''	n	$\alpha(cm^{-1})$
0.297		14.48	0.53		0.0044
0.466		14.11	0.78		0.010
0.615		14.34	0.74		0.012_7
0.86		14.24	1.03		0.024_6
1.22		13.70	1.89		0.065_2
1.80		13.21	2.86		0.148
2.26		12.99	3.53		0.230
3.41		11.66	4.54		0.466
8.32		8.01	5.45		1.65
13.75		5.82	4.35		2.53
29.64		3.91	2.67		5.38
54.90		3.35	2.05		6.65
54.90		3.33	2.01		6.53
89.18		2.77	1.17		6.78
126.26		2.77	1.01		8.04
5.23	174			1.525	
9.39	313			1.521	
13.55	452			1.572	
14.40	480			1.548	2.88
64.50	2150			1.492	2.17
84.00	2800			1.47_8	2.12
100.5	3350			1.458	0.67
115.5	3850			1.464	0.74
123.0	4100			1.442	2.03
130.5	4350			1.443	1.75
141.0	4700			1.430	0.21
509.08	16969			1.4438	

Table I (continued)

Ethylene carbonate - $CHC\ell_3$ mixture $X_{EC} = 0.234$ $C_{EC} = 3.01$ M

f(THz)	$\bar{\nu}(cm^{-1})$	ϵ'	ϵ''	n	$\alpha(cm^{-1})$
0.297×10^{-3}		19.60	0.905		0.0064
0.466×10^{-3}		19.27	1.29		0.0144
0.615×10^{-3}		19.05	1.22		0.0180
0.860×10^{-3}		18.79	2.21		0.0460
1.22×10^{-3}		18.98	3.60		0.105
1.80×10^{-3}		18.72	5.18		0.223
2.24×10^{-3}		17.85	6.27		0.343
3.40×10^{-3}		15.99	7.98		0.691
8.32×10^{-3}		7.16	8.28		2.47
13.75×10^{-3}		3.98	6.32		3.70
29.63×10^{-3}		3.12	4.10		6.58
$54.7_0 \times 10^{-3}$		3.00	2.52		8.32
$88.7_3 \times 10^{-3}$		2.92	1.26		7.04
126.1×10^{-3}		2.78	1.23		9.63
5.10	170			1.523	
7.50	250				8.58
13.62	454			1.569	2.01
16.41	547				1.65
101.9	3395			1.446	1.16
119.3	3978			1.441	1.49
139.9	4662			1.426	0.149
509.08	16969			1.4436	

Table I (continued)

Ethylene carbonate - $CHC\ell_3$ X_{EC} = 0.234 C_{EC} = 3.01 M

Additional values of the attenuation coefficient $\alpha(cm^{-1})$ in the far IR region encompassing the maximum in attenuation

f(THz)	$\bar{\nu}(cm^{-1})$	$\alpha(cm^{-1})$
5.40	180	4.50
6.00	199.9	8.71
6.11	203.8	15.1_6
6.31	210.2	19.5_1
6.36	212.1	18.83
6.42	214.0	18.58
6.48	216.0	17.85
6.60	219.8_5	13.23
7.50	250.0_6	6.55

Table II

Static permittivity ϵ_o (measured at 1.1 MHz by a resonant method) of dimethylcarbonate-chloroform and ethylene carbonate-chloroform mixtures at 25°C.

DMC-$CHC\ell_3$

C_{DMC}	X_{DMC}	ϵ_o [a]
0	0	4.72
0.624	0.051	4.66
1.38	0.113	4.49
3.23	0.267	4.28
4.89	0.409	4.12
5.97	0.495	4.05
6.80	0.565	3.77
8.44	0.705	3.59
9.25	0.776	3.54
10.73	0.909	3.27
11.87	1.00	3.12

[a] $\epsilon_o = 4.72_4 - 1.574\ X_{DMC}$; $r^2 = 0.992$

Ethylene carbonate-$CHC\ell_3$

C_{EC}	X_{EC}	ϵ_o [b]
0	0	4.72
0.529	0.0423	7.07
1.00	0.0789	9.23
3.01	0.234	19.95
4.50	0.341	26.92
6.03	0.433	34.49
7.52	0.531	43.11
9.31	0.643	52.86

[b] up to $C_{EC} = 9.31$ mol/dm^3

$\epsilon_o = 4.65_9 + 57.26\ X_{EC} + 26.39\ X_{EC}^2 + 2.12\ X_{EC}^3$; $r^2 = 0.9998$

Table III

Dielectric parameters ϵ_o, ϵ_∞, f_r and α (where applicable) according to the Debye ($\alpha = 0$) and Cole-Cole function ($\alpha > 0$) and ϵ_o, $\epsilon_{\infty 1}$, $\epsilon_{\infty 2}$, f_1, f_2 according to the sum of two Debye functions. These parameters were obtained by optimum fit of the microwave complex permittivity $\epsilon^* = \epsilon' - J\epsilon''$ investigated at frequencies between 1.1 and 126 GHz at 25°C, and for the indicated solvent systems.

Liquid system	ϵ_o	ϵ_∞	f_r (GHz)	α	Function
DMC	3.12	2.35	22	0	Debye
$CHC\ell_3$	4.719*	2.26	27	0	Debye
DMC - $CHC\ell_3$ $X_{DMC} = 0.268$; $C_{DMC} = 3.23$	4.28	2.22	21	0.08	Cole-Cole
DMC - $CHC\ell_3$ $X_{DMC} = 0.494$; $C_{DMC} = 5.95$	4.05	2.30	17	0.08	Cole-Cole
DMC - $CHC\ell_3$ $X_{DMC} = 0.781$; $C_{DMC} = 9.25$	3.54	2.26	18	0.08	Cole-Cole
DMC-$CC\ell_4$ $X_{DMC} = 0.51$ $C_{DMC} = 5.60$	2.57	2.24	22	0	Debye

* Ref 4

Table III (continued)

Liquid System	ϵ_o	$\epsilon_{\infty 1}$	$\epsilon_{\infty 2}$	f_1	f_2	α	function
EC-$CHC\ell_3$	7.07	4.10	2.25	8.0	32	0	2 Debyes
X_{EC} = 0.0423 C_{EC} = 0.529							
EC-$CHC\ell_3$	9.23	4.00	2.25	7.5	27	0	2 Debyes
X_{EC} = 0.0787 C_{EC} = 1.00							
EC-$CHC\ell_3$	14.30	3.90	2.50	6.8	32	0	2 Debyes
X_{EC} = 0.156 C_{EC} = 2.00							
EC-$CHC\ell_3$	19.95		2.25	6.2		0	1 Debye
X_{EC} = 0.234 C_{EC} = 3.01							

Figure Captions:

Fig. 1a Reflected power interferogram vs liquid depth ℓ for chloroform at f = 126 GHz and 25°C filling a waveguide cell confined by a mica window and a metal reflector.

Fig. 1B Plot of $\ln(\Gamma - \Gamma_\infty)/(1 - \Gamma\Gamma_\infty)$ vs odd values of n and of $\ln(\Gamma_\infty \pm \Gamma)/(1 \pm \Gamma\Gamma_\infty)$ vs even values of n for chloroform at 25°C. Γ and Γ_∞ are the power reflection coefficient at distance ℓ and ∞ respectively from the mica air to liquid separation window. N is the number of quarter wavelengths in the interferogram.

Fig. 2 Real part of the complex permittivity ϵ' for dimethylcarbonate at 25°C vs the frequency f ranging from radio frequencies to optical frequencies.

Fig. 3 Cole-Cole plot of ϵ'' vs ϵ' for dimethylcarbonate at 25°C extended to the value of the Na-doublet at optical frequencies.

Fig. 4 Attenuation constant $\alpha(cm^{-1})$ vs the frequency f(THz) and wavenumber $\bar{\nu}(cm^{-1})$ for DMC at 25°C showing a maximum at far infrared frequencies.

Fig. 5 Real part of the dielectric permittivity ϵ' vs the frequency f(THz) and vs the wavenumber $\bar{\nu}(cm^{-1})$ for $CHC\ell_3$ at 25°C.

Fig. 6 Attenuation constant $\alpha(cm^{-1})$ vs the frequency f(THz) and wavenumber $\bar{\nu}(cm^{-1})$ for $CHC\ell_3$ at 25°C, showing a maximum at far infrared frequencies.

Fig. 7 (microfilm edition) Cole-Cole plot for the mixture DMC-$CHC\ell_3$ of composition X_{DMC} = 0.50 (C_{DMC} = 5.95 M), showing ϵ'' vs ϵ' at 25°C. The solid line is the interpretation according to a Cole-Cole distribution of relaxation times with parameters ϵ_o = 4.05, ϵ_∞ = 2.30, f_r = 17 GHz and a distribution parameter α = 0.08.

Fig. 8 (microfilm edition) Cole-Cole plot for the mixture DMC-$CC\ell_4$ of composition X_{DMC} = 0.50 (C_{DMC} = 5.60 M) showing ϵ'' vs ϵ' at 25°C. The solid line corresponds to a single Debye relaxation with parameters ϵ_o = 2.57, ϵ_∞ = 2.24, f_r = 22 GHz.

Fig. 9A Average dielectric relaxation time $\bar{\tau}_D$ (picoseconds) vs composition, X_{DMC} for DMC-$CHC\ell_3$ mixtures at 25°C.

Fig. 9B Relaxation strength ($\epsilon_o - \epsilon_\infty$) vs composition, X_{DMC} for DMC-$CHC\ell_3$ mixtures at 25°C.

Fig. 10A Attenuation constant $\alpha(cm^{-1})$ vs frequency f(THz) and vs wavenumber $\bar{\nu}(cm^{-1})$ for DMC in $CC\ell_4$ at X_{DMC} = 0.509 (C_{DMC} = 5.60 M) and 25°C.

Fig. 10B Attenuation constant $\alpha(cm^{-1})$ vs frequency f(THz) and vs wavenumber $\bar{\nu}(cm^{-1})$ for DMC in $CHC\ell_3$ at X_{DMC} = 0.491 (C_{DMC} = 5.86 M) and 25°C.

Fig. 11 A,B,C,D Cole-Cole plots of ethylene carbonate-$CHC\ell_3$ mixtures at concentrations of ethylene carbonate C = 0.529 M (A); C = 1.00 M (B); C = 2.00 M (C); C = 3.01 M (D)

Fig. 11 E Böttcher plot of ethylene carbonate in chloroform at 25°C.

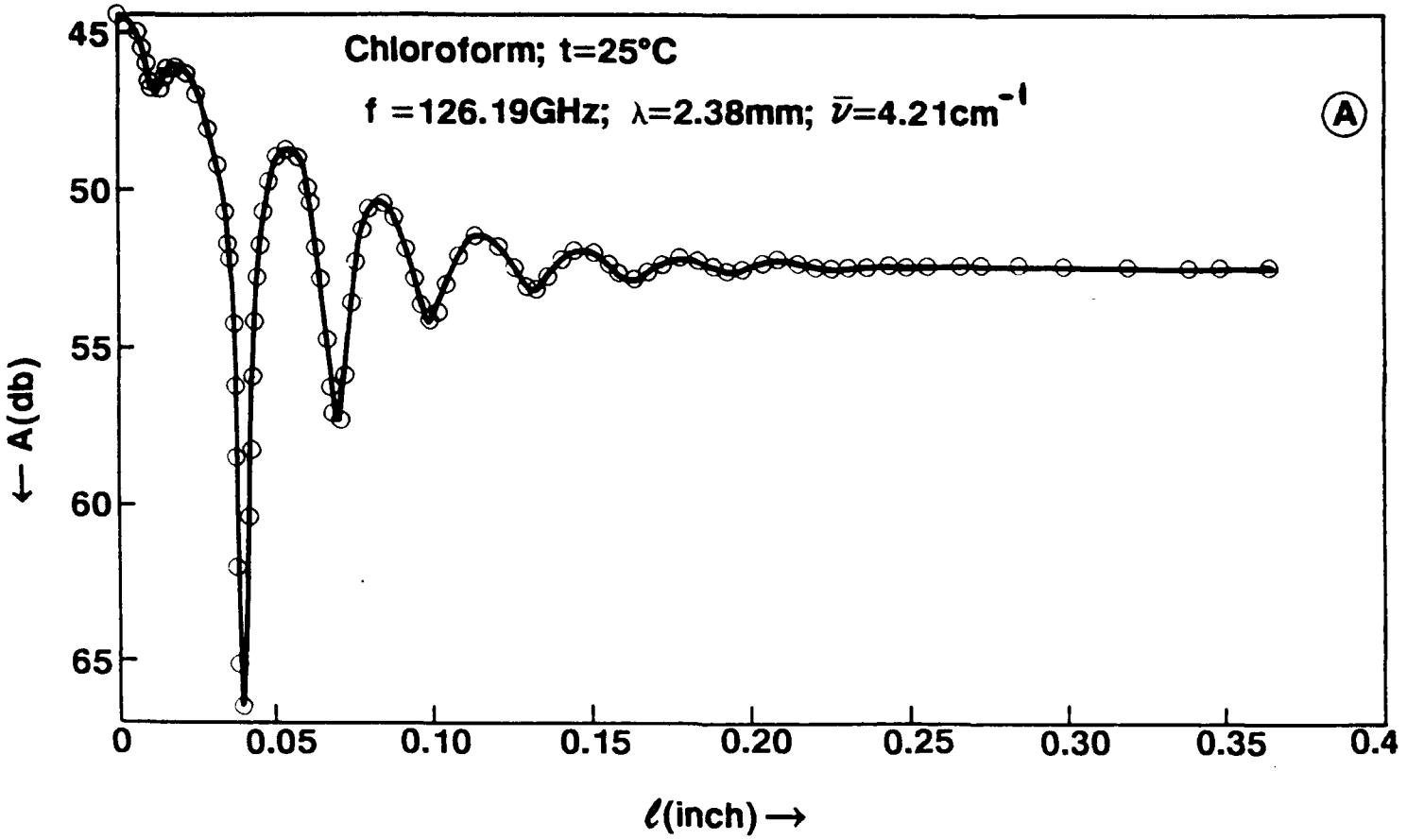
Chloroform; t=25°C
f =126.19GHz; λ=2.38mm; $\bar{\nu}$=4.21cm^{-1}
A
45
50
55
60
65
← A(db)
0
0.05
0.10
0.15
0.20
0.25
0.30
0.35
0.4
ℓ(inch) →

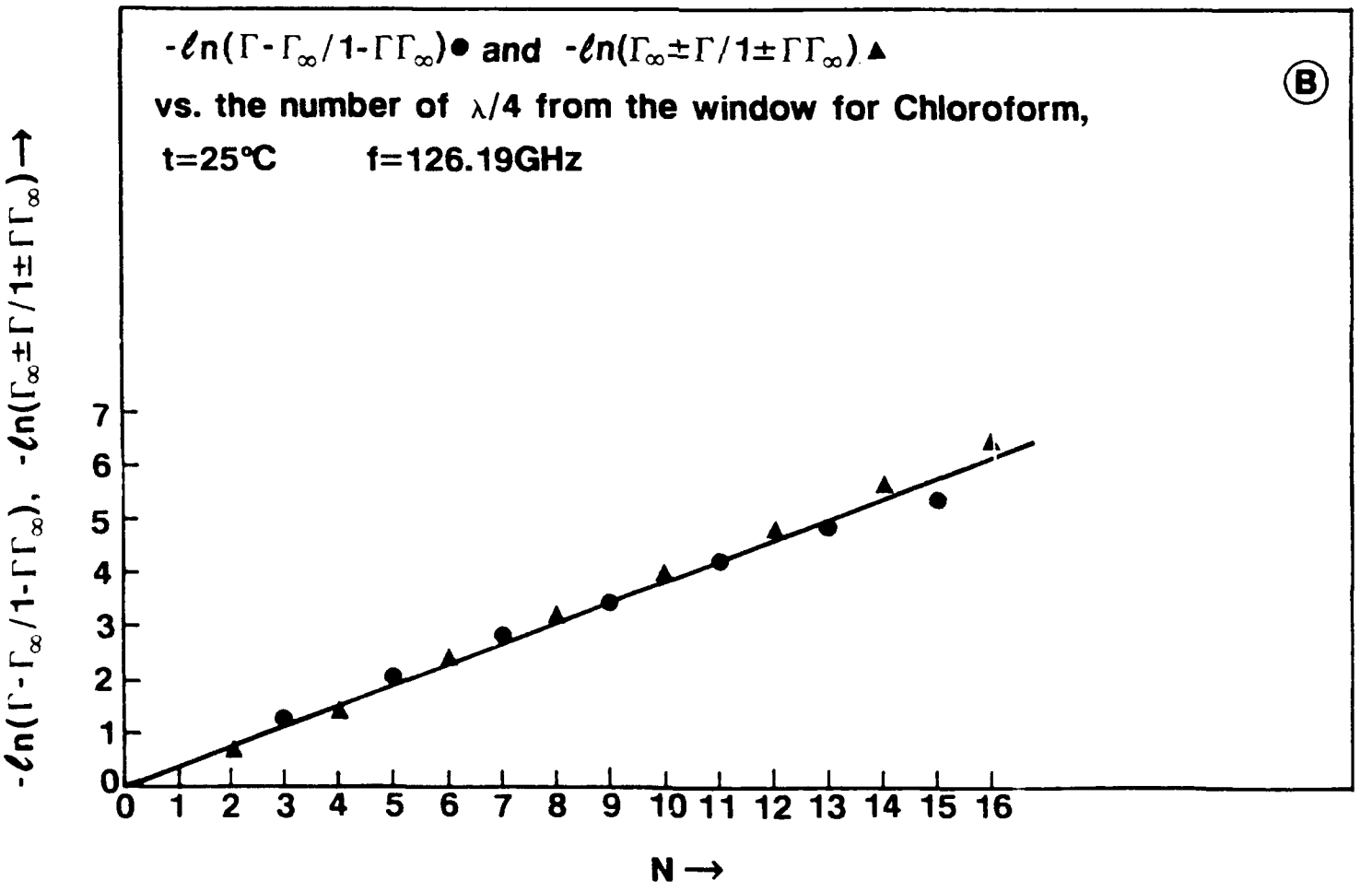
$-\ell n(\Gamma-\Gamma_\infty/1-\Gamma\Gamma_\infty)$● and $-\ell n(\Gamma_\infty\pm\Gamma/1\pm\Gamma\Gamma_\infty)$▲
vs. the number of λ/4 from the window for Chloroform,
t=25°C f=126.19GHz
B
$-\ell n(\Gamma-\Gamma_\infty/1-\Gamma\Gamma_\infty)$, $-\ell n(\Gamma_\infty\pm\Gamma/1\pm\Gamma\Gamma_\infty)$ →
0
1
2
3
4
5
6
7
0 1 2 3 4 5 6 7 8 9 10 11 12 13 14 15 16
N →

Fig. 1

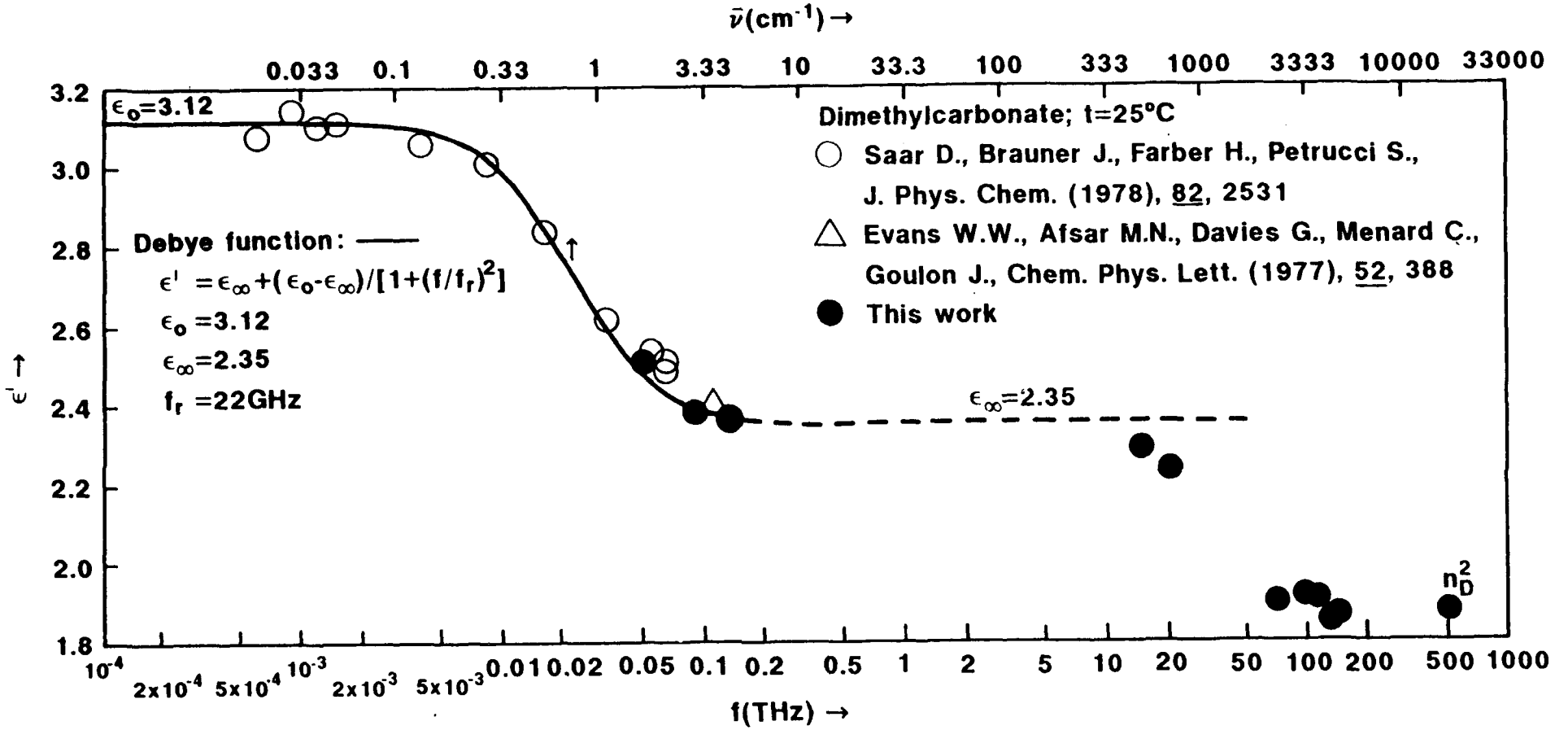
$\bar{\nu}$(cm^{-1})→
0.033 0.1 0.33 1 3.33 10 33.3 100 333 1000 3333 10000 33000
3.2
3.0
2.8
2.6
2.4
2.2
2.0
1.8
ϵ_o=3.12
Dimethylcarbonate; t=25°C
Saar D., Brauner J., Farber H., Petrucci S., J. Phys. Chem. (1978), 82, 2531
Evans W.W., Afsar M.N., Davies G., Menard Ç., Goulon J., Chem. Phys. Lett. (1977), 52, 388
This work
Debye function: ——
$\epsilon' = \epsilon_\infty + (\epsilon_o - \epsilon_\infty)/[1+(f/f_r)^2]$
ϵ_o =3.12
ϵ_∞=2.35
f_r =22GHz
ϵ_∞=2.35
n_D^2
ϵ' ↑
10^{-4} 2×10^{-4} 5×10^{-4} 10^{-3} 2×10^{-3} 5×10^{-3} 0.01 0.02 0.05 0.1 0.2 0.5 1 2 5 10 20 50 100 200 500 1000
f(THz) →

Fig. 2

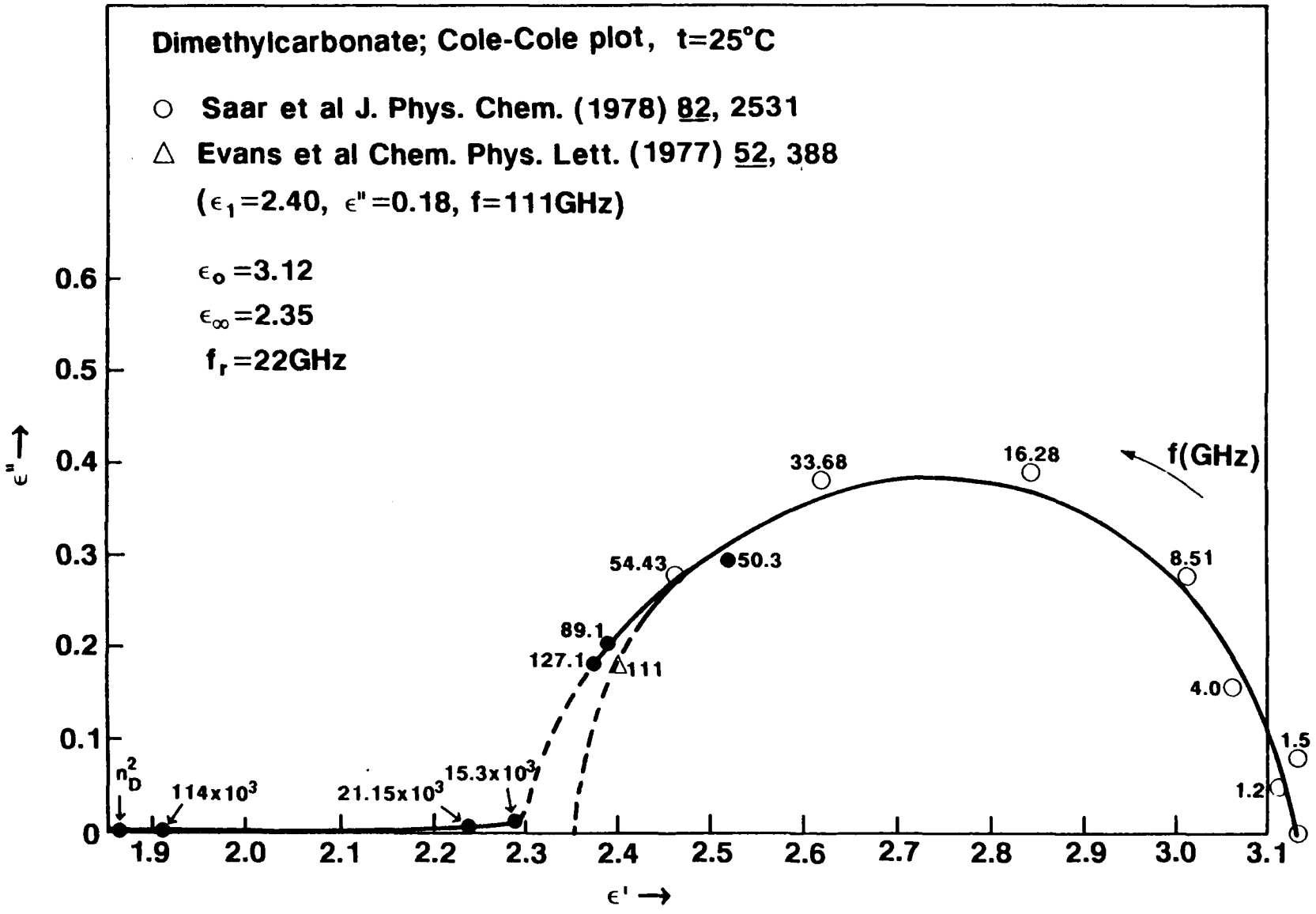
Dimethylcarbonate; Cole-Cole plot, t=25°C
○ Saar et al J. Phys. Chem. (1978) 82, 2531
△ Evans et al Chem. Phys. Lett. (1977) 52, 388
(ε1=2.40, ε"=0.18, f=111GHz)
εo=3.12
ε∞=2.35
fr=22GHz
ε" ↑
ε' →
f(GHz)
33.68
16.28
54.43
50.3
8.51
89.1
127.1
111
4.0
1.5
1.2
n²D
114x10³
21.15x10³
15.3x10³
0.6
0.5
0.4
0.3
0.2
0.1
0
1.9
2.0
2.1
2.2
2.3
2.4
2.5
2.6
2.7
2.8
2.9
3.0
3.1

Fig. 3

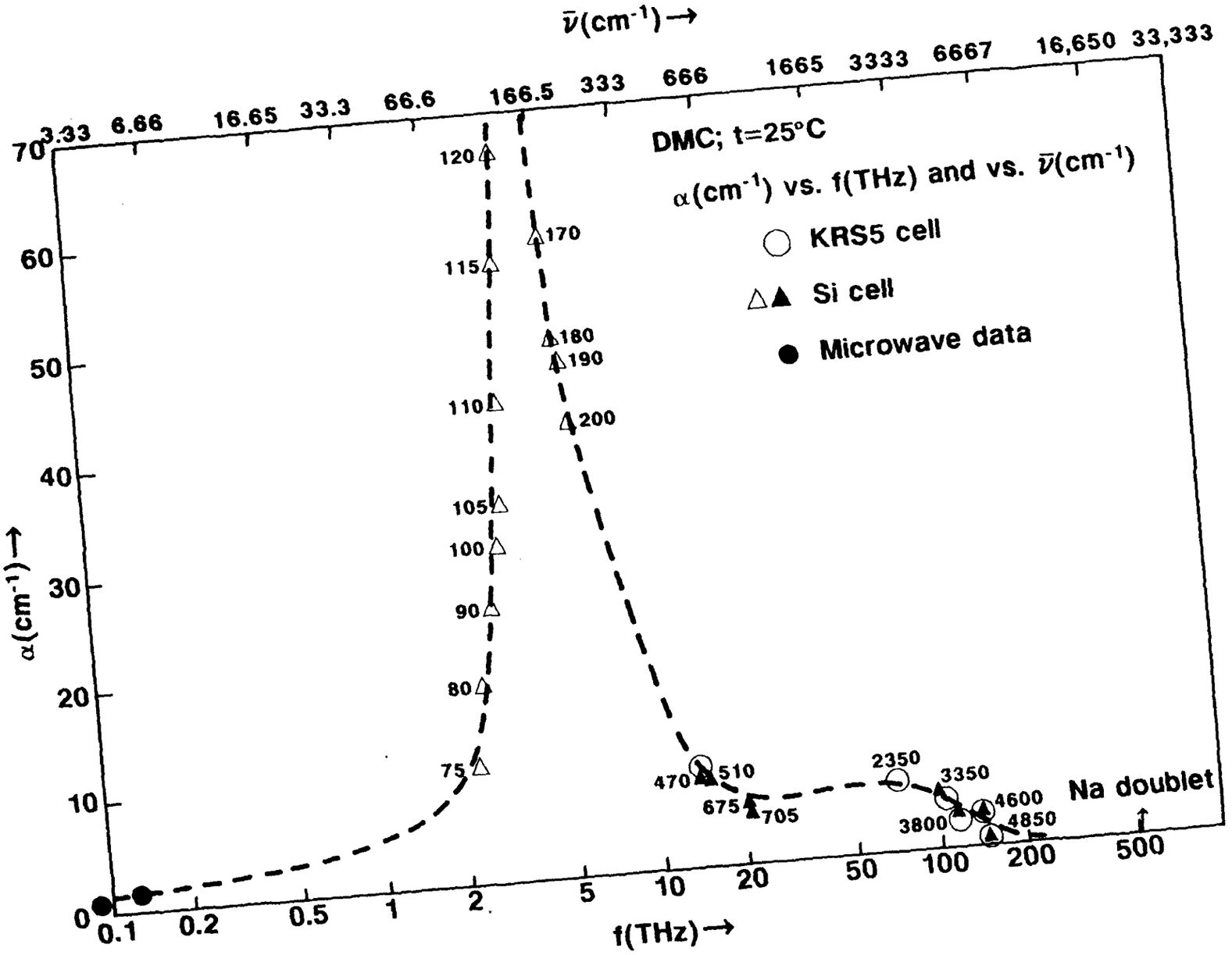
$\bar{\nu}(cm^{-1})\rightarrow$
3.33 6.66 16.65 33.3 66.6 166.5 333 666 1665 3333 6667 16,650 33,333
DMC; t=25°C
$\alpha(cm^{-1})$ vs. f(THz) and vs. $\bar{\nu}(cm^{-1})$
KRS5 cell
Si cell
Microwave data
120
115
110
105
100
90
80
75
170
180
190
200
470
510
675
705
2350
3350
3800
4600
4850
Na doublet
$\alpha(cm^{-1})\rightarrow$
0 10 20 30 40 50 60 70
0.1 0.2 0.5 1 2 5 10 20 50 100 200 500
f(THz)→

Fig 7

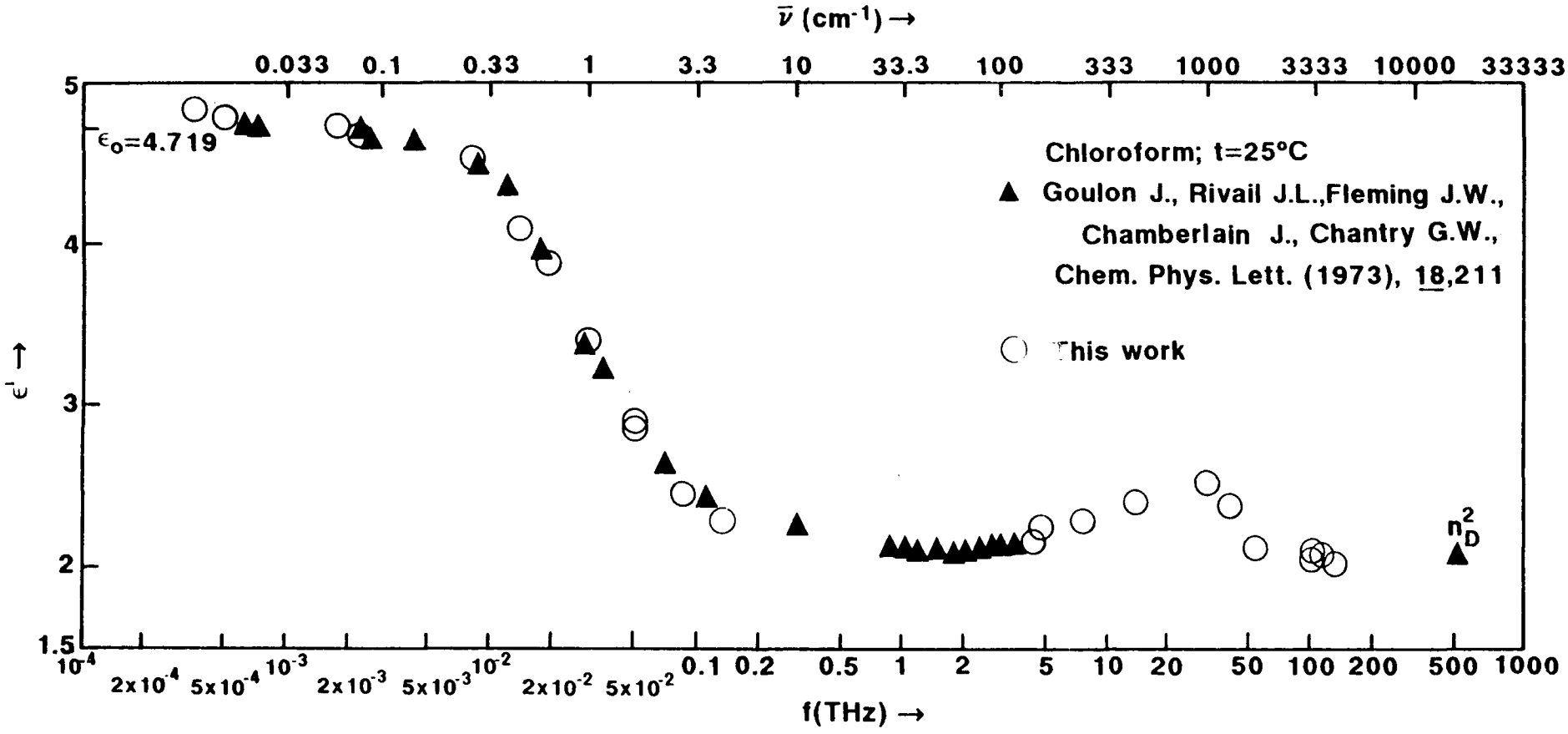
$\bar{\nu}$ (cm^{-1}) →
0.033 0.1 0.33 1 3.3 10 33.3 100 333 1000 3333 10000 33333
ϵ_o=4.719
Chloroform; t=25°C
Goulon J., Rivail J.L.,Fleming J.W.,
Chamberlain J., Chantry G.W.,
Chem. Phys. Lett. (1973), 18,211
This work
n_D^2
ϵ' ↑
5
4
3
2
1.5
10^{-4} 2×10^{-4} 5×10^{-4} 10^{-3} 2×10^{-3} 5×10^{-3} 10^{-2} 2×10^{-2} 5×10^{-2} 0.1 0.2 0.5 1 2 5 10 20 50 100 200 500 1000
f(THz) →

Fig. 15

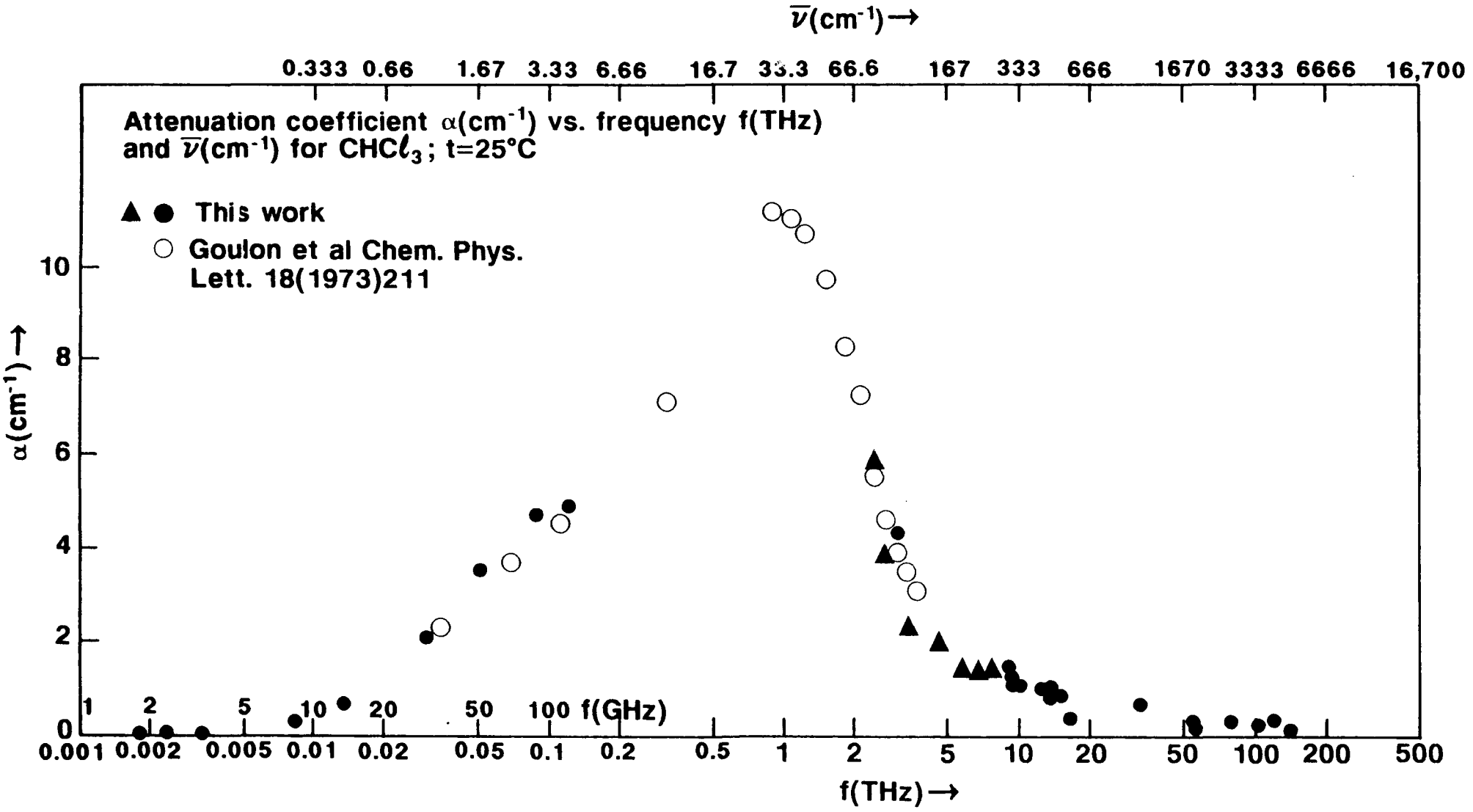
$\overline{\nu}$(cm^{-1})→
0.333 0.66 1.67 3.33 6.66 16.7 33.3 66.6 167 333 666 1670 3333 6666 16,700
Attenuation coefficient α(cm^{-1}) vs. frequency f(THz)
and $\overline{\nu}$(cm^{-1}) for CHCℓ$_3$; t=25°C
▲ ● This work
○ Goulon et al Chem. Phys. Lett. 18(1973)211
α(cm^{-1})→
0 2 4 6 8 10
1 2 5 10 20 50 100 f(GHz)
0.001 0.002 0.005 0.01 0.02 0.05 0.1 0.2 0.5 1 2 5 10 20 50 100 200 500
f(THz)→

Fig. 6

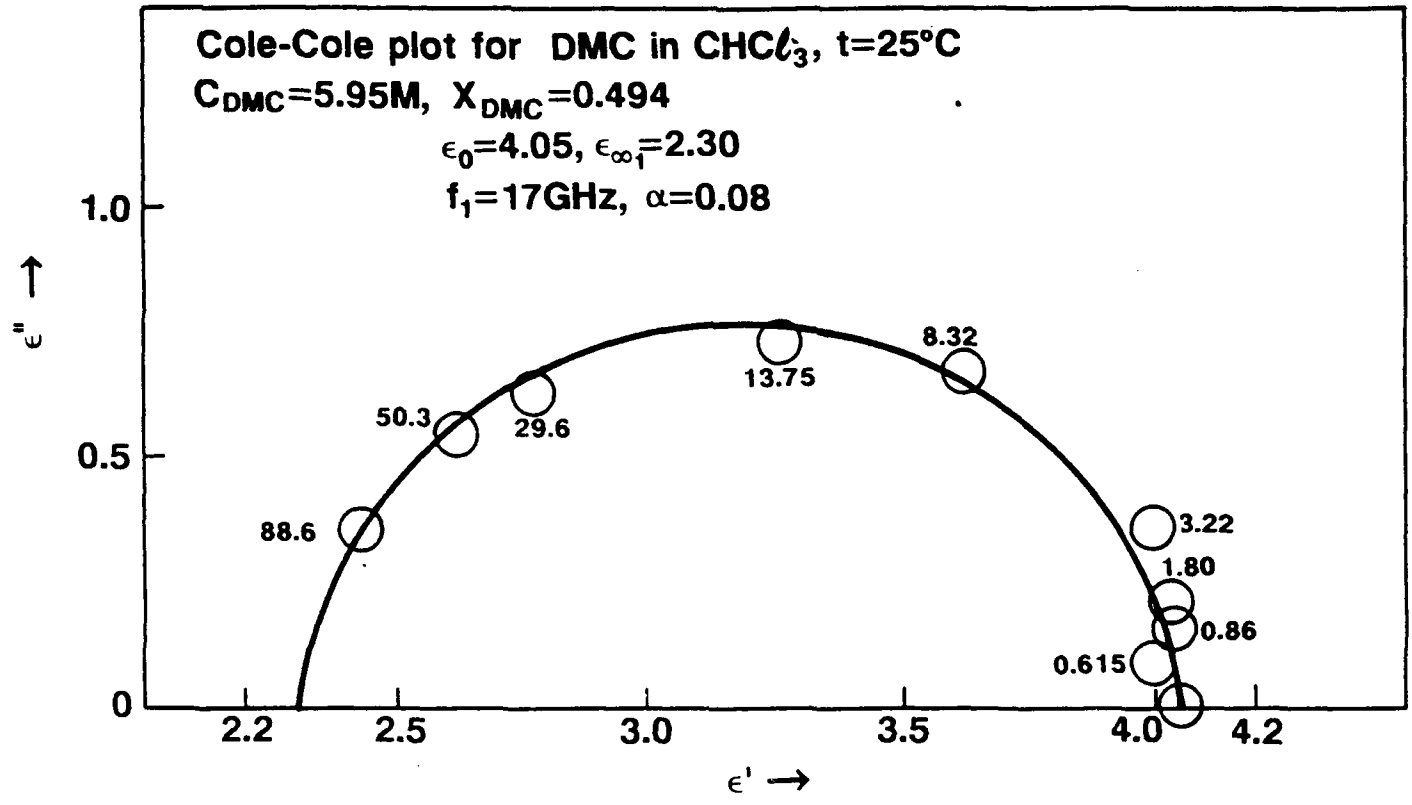

microwave edition

Fig 7

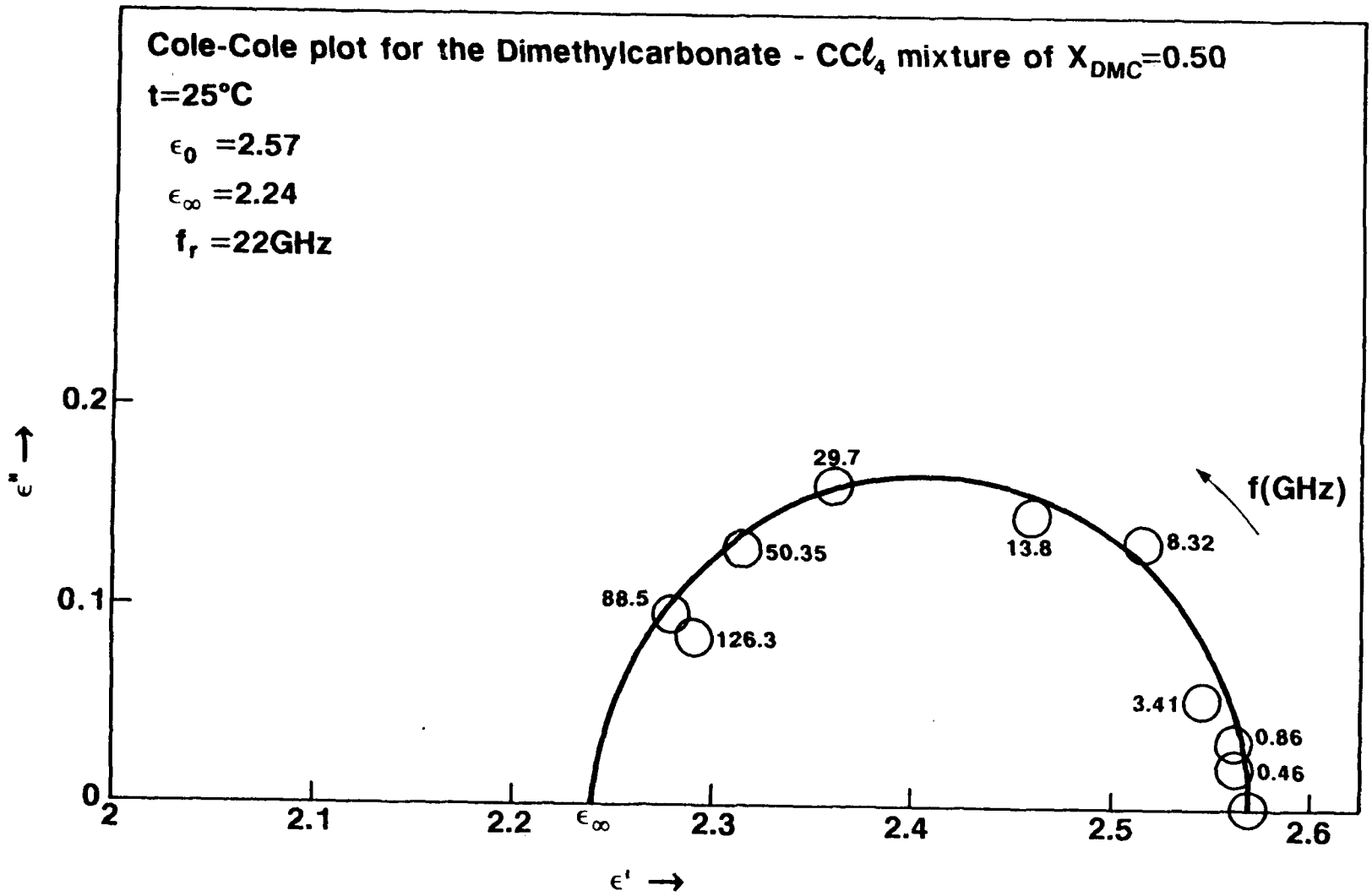
Cole-Cole plot for the Dimethylcarbonate - CCℓ4 mixture of XDMC=0.50
t=25°C
ε0 =2.57
ε∞ =2.24
fr =22GHz
0.2
0.1
0
ε" ↑
29.7
50.35
88.5
126.3
13.8
8.32
3.41
0.86
0.46
f(GHz)
2
2.1
2.2
ε∞
2.3
2.4
2.5
2.6
ε' →

Fig 8

[illegible]

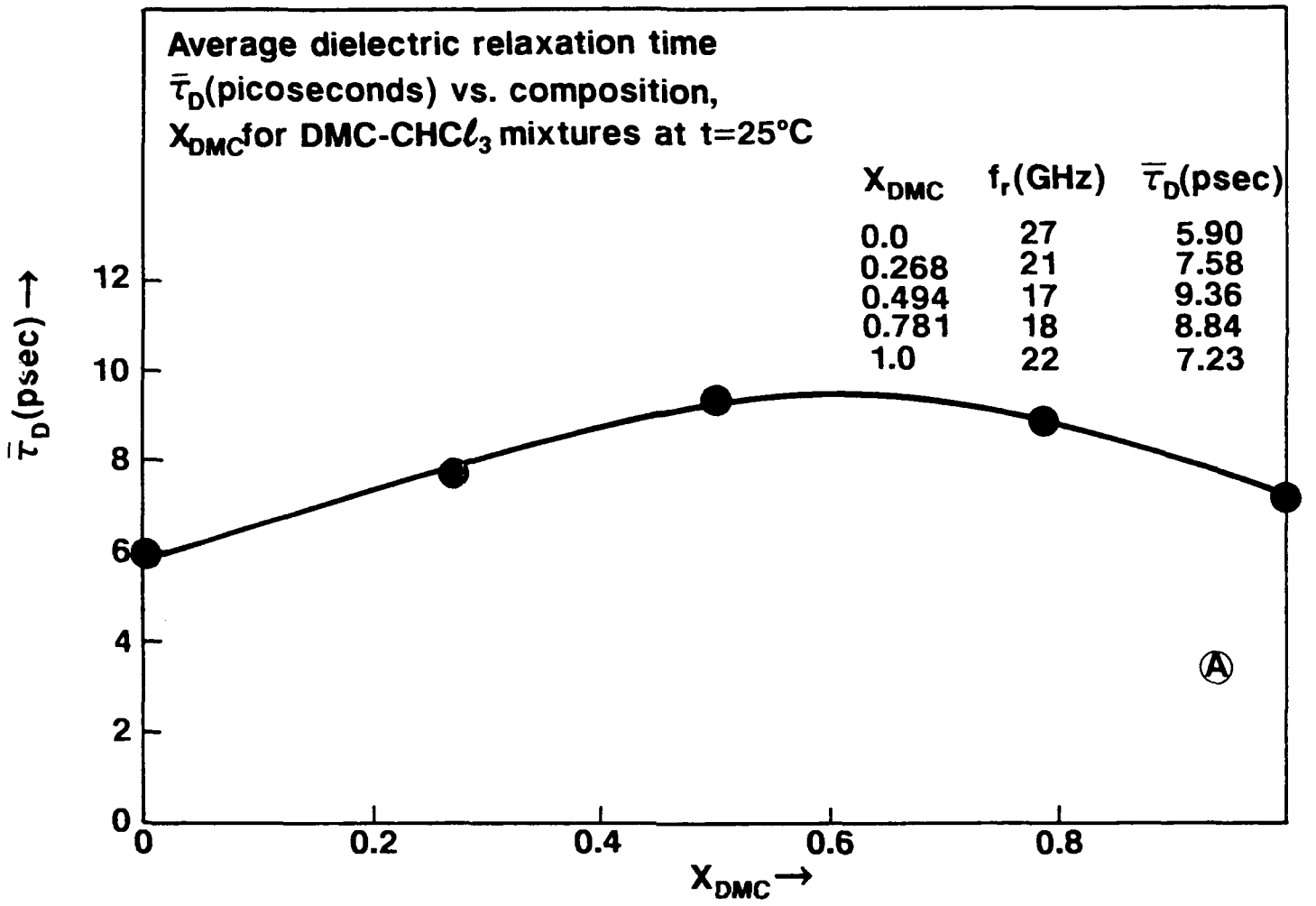
Average dielectric relaxation time
$\bar{\tau}_D$(picoseconds) vs. composition,
X_{DMC} for DMC-$CHC\ell_3$ mixtures at t=25°C
X_{DMC} f_r(GHz) $\bar{\tau}_D$(psec)
0.0 27 5.90
0.268 21 7.58
0.494 17 9.36
0.781 18 8.84
1.0 22 7.23
$\bar{\tau}_D$(psec) →
0
2
4
6
8
10
12
0
0.2
0.4
0.6
0.8
X_{DMC} →
Ⓐ

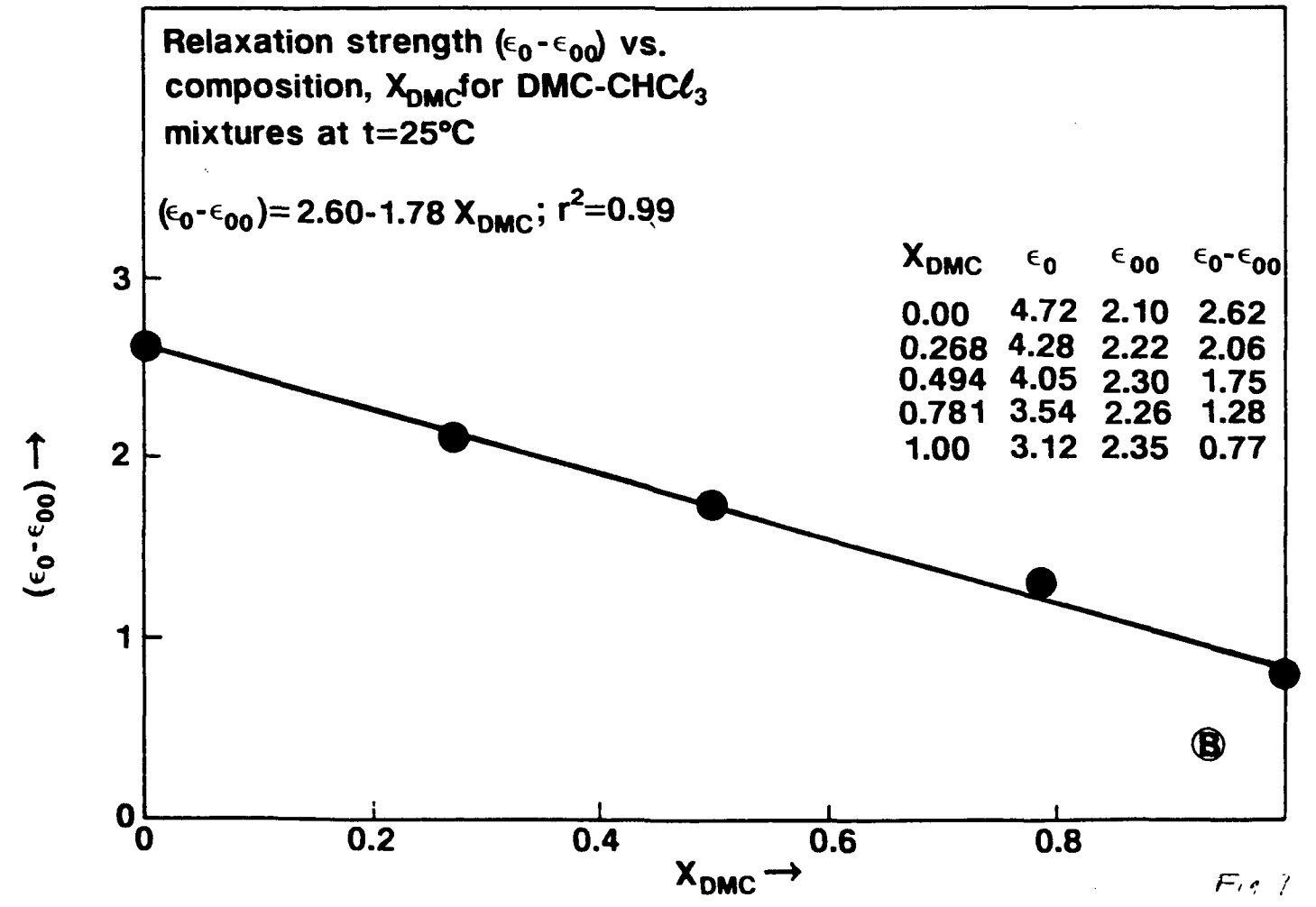
Relaxation strength (ϵ_0-ϵ_{00}) vs.
composition, X_{DMC} for DMC-$CHC\ell_3$
mixtures at t=25°C
(ϵ_0-ϵ_{00})= 2.60-1.78 X_{DMC}; r^2=0.99
X_{DMC} ϵ_0 ϵ_{00} ϵ_0-ϵ_{00}
0.00 4.72 2.10 2.62
0.268 4.28 2.22 2.06
0.494 4.05 2.30 1.75
0.781 3.54 2.26 1.28
1.00 3.12 2.35 0.77
(ϵ_0-ϵ_{00}) →
0
1
2
3
0
0.2
0.4
0.6
0.8
X_{DMC} →
Ⓑ

Fig 1

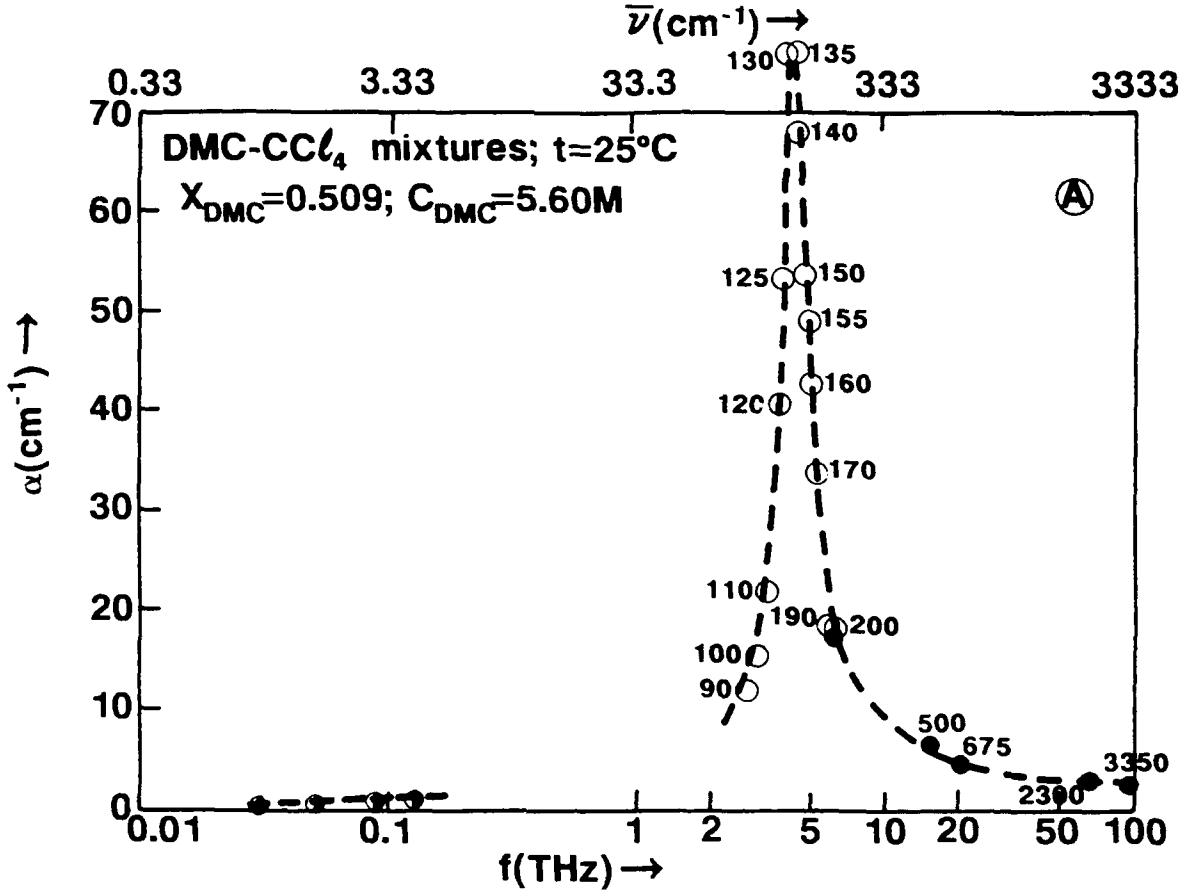
$\bar{\nu}$(cm^{-1})→
0.33
3.33
33.3
333
3333
DMC-CCℓ$_4$ mixtures; t=25°C
X_{DMC}=0.509; C_{DMC}=5.60M
Ⓐ
α(cm^{-1})→
f(THz)→
0.01
0.1
1
2
5
10
20
50
100
0
10
20
30
40
50
60
70
90
100
110
120
125
130
135
140
150
155
160
170
190
200
500
675
2300
3350

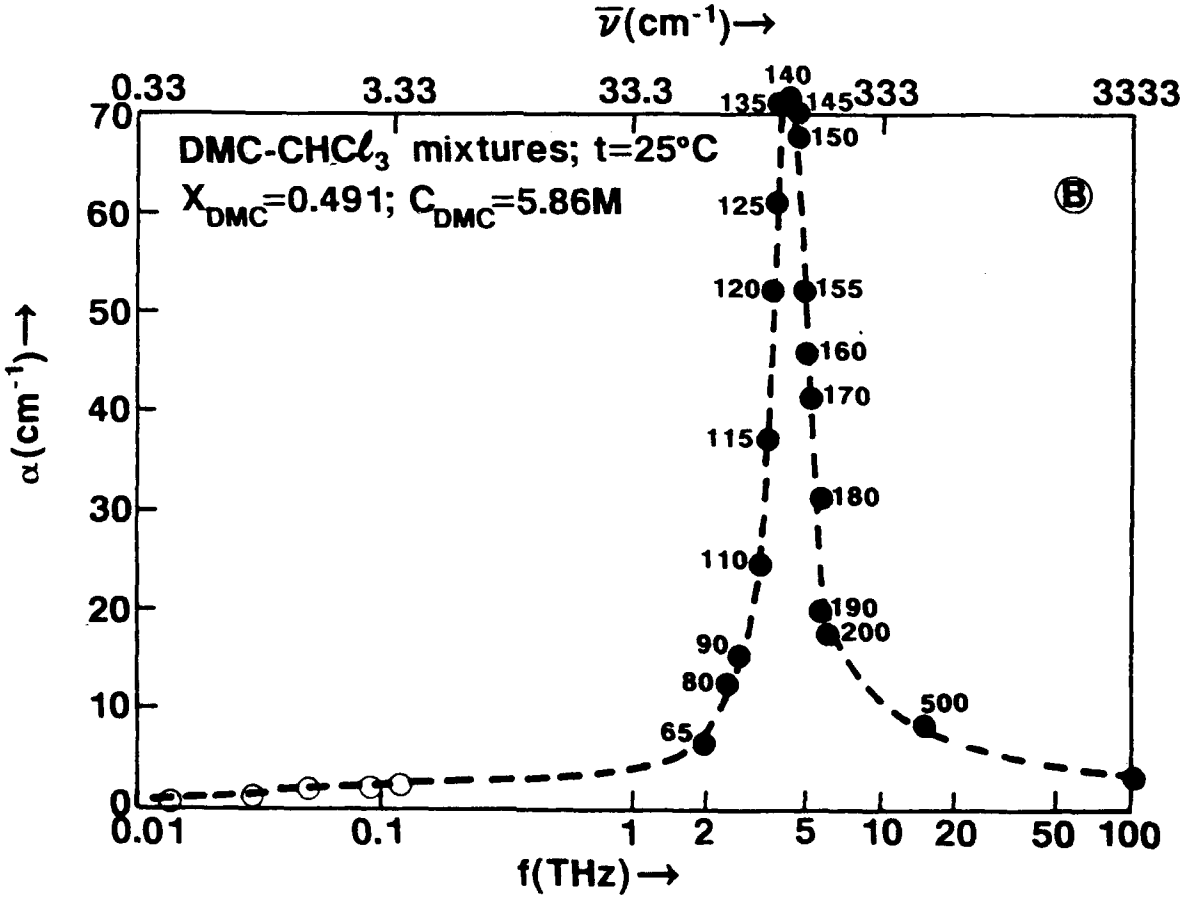
$\bar{\nu}$(cm^{-1})→
0.33
3.33
33.3
333
3333
DMC-CHCℓ$_3$ mixtures; t=25°C
X_{DMC}=0.491; C_{DMC}=5.86M
Ⓑ
α(cm^{-1})→
f(THz)→
0.01
0.1
1
2
5
10
20
50
100
0
10
20
30
40
50
60
70
65
80
90
110
115
120
125
135
140
145
150
155
160
170
180
190
200
500

Fig 10

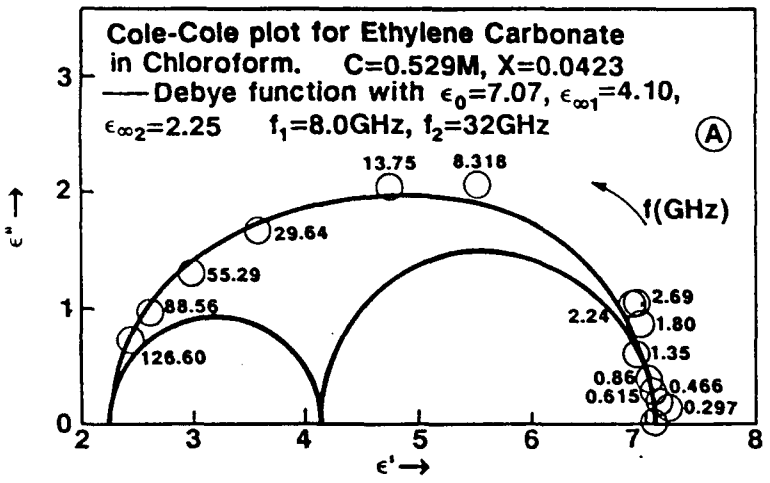
Cole-Cole plot for Ethylene Carbonate
in Chloroform. C=0.529M, X=0.0423
—— Debye function with ϵ_0=7.07, $\epsilon_{\infty 1}$=4.10,
$\epsilon_{\infty 2}$=2.25 f_1=8.0GHz, f_2=32GHz
A
f(GHz)
13.75
8.318
29.64
55.29
88.56
126.60
2.69
2.24
1.80
1.35
0.86
0.615
0.466
0.297
ε''→
ε'→

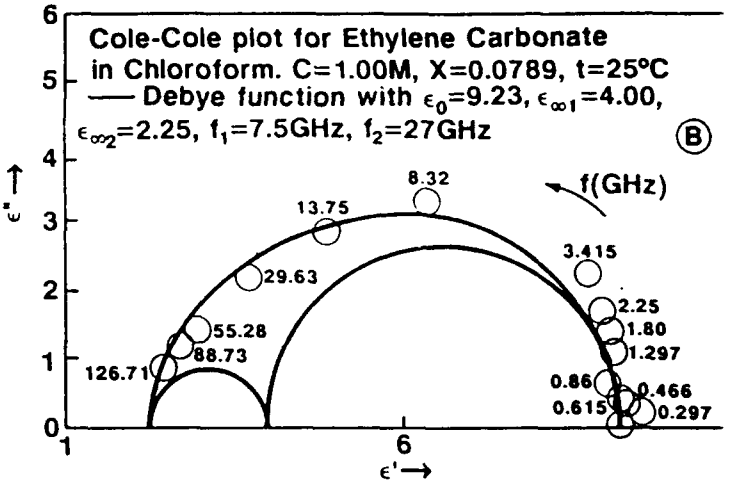
Cole-Cole plot for Ethylene Carbonate
in Chloroform. C=1.00M, X=0.0789, t=25°C
—— Debye function with ϵ_0=9.23, $\epsilon_{\infty 1}$=4.00,
$\epsilon_{\infty 2}$=2.25, f_1=7.5GHz, f_2=27GHz
B
f(GHz)
8.32
13.75
29.63
3.415
55.28
88.73
126.71
2.25
1.80
1.297
0.86
0.615
0.466
0.297
ε''→
ε'→

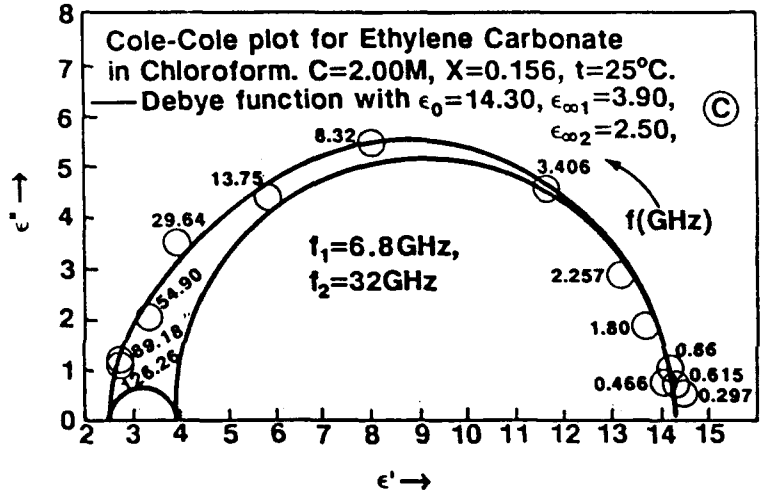
Cole-Cole plot for Ethylene Carbonate
in Chloroform. C=2.00M, X=0.156, t=25°C.
—— Debye function with ϵ_0=14.30, $\epsilon_{\infty 1}$=3.90,
$\epsilon_{\infty 2}$=2.50,
C
8.32
13.75
29.64
54.90
89.18
126.26
3.406
f(GHz)
f_1=6.8GHz,
f_2=32GHz
2.257
1.80
0.86
0.615
0.466
0.297
ε''→
ε'→

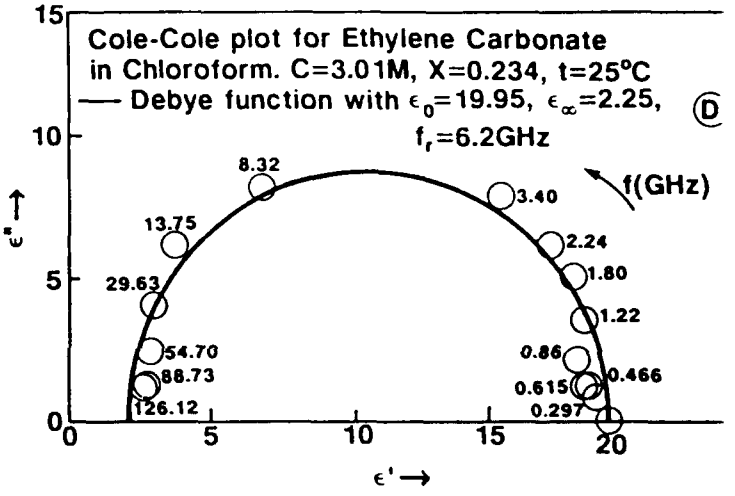
Cole-Cole plot for Ethylene Carbonate
in Chloroform. C=3.01M, X=0.234, t=25°C
—— Debye function with ϵ_0=19.95, ϵ_∞=2.25,
f_r=6.2GHz
D
8.32
3.40
f(GHz)
13.75
29.63
54.70
88.73
126.12
2.24
1.80
1.22
0.86
0.615
0.466
0.297
ε''→
ε'→

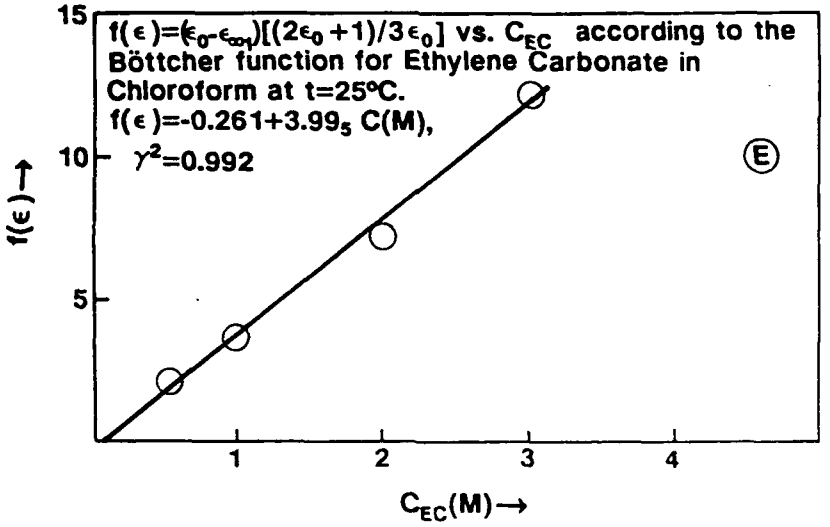
$f(\epsilon)=(\epsilon_0-\epsilon_{\infty 1})[(2\epsilon_0+1)/3\epsilon_0]$ vs. C_{EC} according to the
Böttcher function for Ethylene Carbonate in
Chloroform at t=25°C.
$f(\epsilon)=-0.261+3.99_5\ C(M)$,
γ^2=0.992
E
f(ε)→
C_{EC}(M)→

Fig 11